accomplished, the resulting mutant receptor (275*Ala*)-ERRγ was found to exhibit sufficient specific binding (approximately 55% of the total binding) for [^{3}H]BPA (Fig. 3B). In addition, (316*Ala*)-ERRγ with the Arg316 → Ala substitution exhibited barely sufficient specific binding (approimately 40% of the total binding) for [^{3}H]BPA (Fig. 3C), although much higher concentrations of [^{3}H]BPA were required.

When the Glu275 → Ala substitution was accomplished, the resulting mutant receptor (275*Ala*)-ERRγ was found to exhibit considerably decreased binding potency for BPA. Given the absence of a carboxymethyl group of Glu275, the binding energy of [^{3}H]BPA to (275*Ala*)-ERRγ was estimated to be considerably weaker than that to wild-type ERRγ. Indeed, it showed significantly diminished binding ability with a dissociation constant of 17.8 nM (32% of the binding affinity for the wild-type ERRγ) (Fig. 4, Table 1).

The Arg316 → Ala substitution resulted in a further diminution of activity (Fig. 4). The dissociation constants were 171 nM (only 3.3% of the binding affinity for the wild-type ERRγ) for [^{3}H]BPA (Fig. 4, Table 1). These results clearly indicate that the hydrogen bonds between the phenol-hydroxyl group of BPA and the Glu275 and Arg316 residues are crucial for capturing BPA in the binding pocket of the ERRγ-LBD. Moreover, it is clear that the hydrogen bond between the BPA and Arg316 is much more important than that between BPA and the Glu275.

Table 1. Receptor binding characteristics of ERRγ and its mutants by [^{3}H]BPA. Specifically mutated residues are shown in italics. NSB, no specific binding in the saturation binding assay.

Amino acid residues of ERRγ receptors		Binding characteristics of [^{3}H]BPA	
Position 275	Position 316	Dissociation constant (K_D, nM)	Receptor density (B_{max}, nmol/mg)
Glu	Arg[a]	5.70 ± 0.88	18.4 ± 0.78
Ala	Arg	17.8 ± 2.74	6.72 ± 0.62
Asp	Arg	22.0 ± 2.86	12.4 ± 0.46
Gln	Arg	23.4 ± 3.34	7.81 ± 0.47
Leu	Arg	NSB	NSB
Glu	*Ala*	171 ± 39.5	0.56 ± 0.09
Glu	*Lys*	22.5 ± 4.26	9.98 ± 0.76
Glu	*Leu*	NSB	NSB
Ala	*Ala*	NSB	NSB
Arg	*Glu*	59.7 ± 6.79	3.66 ± 0.29
Ala	*Glu*	NSB	NSB
Arg	*Ala*	54.3 ± 6.82	3.56 ± 0.38

[a]Wild-type.

Binding affinity of BPA and 4-OHT in competitive receptor binding assays

The receptor binding results obtained here were also revealed by a competitive binding assay, using [^{3}H]BPA as a tracer. We tested the nonradio-labeled BPA and 4-OHT to evaluate their ability to displace [^{3}H]BPA in the ERRγ ligand-binding pocket. The phenol-hydroxyl group of 4-OHT, an estrogen receptor modulator, shares the same site for its binding to ERRγ [20,22]. BPA and 4-OHT elicited almost the same strong binding activity for the wild-type ERRγ (Table 2, Fig. 5). On the other hand, the concentrations for half-maximal inhibition (IC_{50}) of BPA were 35.7 nM for (275*Ala*)-ERRγ, 27% of the binding affinity for the wild-type ERRγ, and 990 nM for (316*Ala*)-ERRγ, only approximately 1% of that for the wild-type (Fig. 5A, Table 2). The values of IC_{50} and K_D essentially reveal their inter-relationship.

The IC_{50} values of 4-OHT were 53.2 nM for (275*Ala*)-ERRγ (25% of that for the wild-type) and 818 nM for (316*Ala*)-ERRγ (1.6%) (Fig. 5B, Table 2). These results indicate clearly that the hydrogen bonding to the Arg316 residue is more important for capturing BPA and 4-OHT than is the bonding to the Glu275 residue in the binding pocket of ERRγ-LBD.

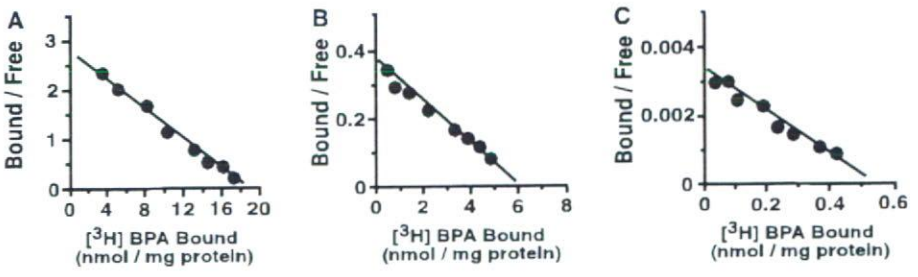

Fig. 4. Scatchard plot analyses showing a single binding mode with a binding affinity constant (K_D) and receptor density (B_{max}). Analyses were carried out from the radioligand receptor saturation binding curves of [^{3}H]BPA for the human ERRγ LBD and its site-directed mutant derivatives. Those include the wild-type ERRγ (A), (275*Ala*)-ERRγ with the Glu275 → Ala substitution (B), and (316*Ala*)-ERRγ with the Arg316 → Ala substitution (C).

Table 2. Receptor binding potency of BPA and 4-OHT in the competitive binding assay for ERRγ and its mutants by [^{3}H]BPA. Specifically mutated residues are shown in italics. Because there was no specific binding in the saturation binding assay, the competitive binding assay could not be carried out. ND, Not determined.

Amino acid residues of ERRγ receptors		Receptor binding potency IC_{50} (nM)	
Position 275	Position 316	BPA	4-OHT
Glu	Arg[a]	9.70 ± 0.59	13.3 ± 3.02
Ala	Arg	35.7 ± 5.48	53.2 ± 10.8
Asp	Arg	36.7 ± 7.18	49.3 ± 8.65
Gln	Arg	52.1 ± 8.99	37.1 ± 5.74
Leu	Arg	ND	ND
Glu	*Ala*	990 ± 184	818 ± 105
Glu	*Lys*	37.1 ± 4.73	54.9 ± 11.3
Glu	*Leu*	ND	ND
Ala	*Ala*	ND	ND
Arg	*Glu*	195 ± 24.5	200 ± 28.8
Ala	*Glu*	ND	ND
Arg	*Ala*	154 ± 32.5	243 ± 17.7

[a]Wild-type.

When Glu275 and Arg316 were each replaced by Leu instead of Ala, the resulting (275*Leu*)-ERRγ and (316*Leu*)-ERRγ mutant receptors were completely inactive, with no specific binding (Table 1). Thus, it was impossible to carry out competitive binding assays for them (Table 2). Because Leu has an additional $-CH(CH_3)_2$ (= isopropyl) group on the β-carbon of the Ala side chain, this hydrophobic bulky group is apparently disadvantageous electrochemically and/or spatially for the interaction with BPA or 4-OHT. Glu has the $-CH_2COOH$ (carboxymethyl) group on the β-carbon of the Ala side chain, whereas Arg has $-CH_2CH_2NHCH(=NH)NH_2$. These groups are capable of making hydrogen bonds with the phenol-hydroxyl group of BPA and also with that of 4-OHT, providing the space that fits the phenol group perfectly.

Replacement of Glu275 and Arg316 with structurally similar amino acids

When Glu275 was replaced solely by glutamine (Gln), with the substitution of the γ-carboxyl (COOH) of Glu to carboxyl amide ($CONH_2$), the resulting (275*Gln*)-ERRγ mutant receptor exhibited a sufficient level of specific binding (approximately 70% of the total binding) for [^{3}H]BPA (data not shown). The K_D values were 23.4 nM (approximately 25% of the binding affinity for the wild-type ERRγ) (Table 1). The IC_{50} values of BPA and 4-OHT were 52.1 nM (19% of the binding affinity for the wild-type) and 37.1 nM (36%), respectively (Table 2). These results are almost equal to those obtained for (275*Ala*)-ERRγ. Thus, the Gln-carboxyl amide ($CONH_2$) group cannot replace the Glu-carboxyl (COOH) group.

In addition to the previous finding, (275*Asp*)-ERRγ with the Glu275 → Asp substitution exhibited a sufficient level of specific binding (approximately 70% of the total binding) for [^{3}H]BPA (data not shown). This mutant receptor (275*Asp*)-ERRγ exhibited only moderate activity levels (30–50%) for BPA and 4-OHT, however, which were similar to those obtained for (275*Ala*)-ERRγ (Tables 1 and 2). Asp with the β-carboxyl group is an acidic amino acid, like Glu, but it lacks the methylene group (CH_2) of Glu at the γ position. All these results indicate that the substitutions of Glu275 with Gln and Asp, and even with Ala, decrease considerably the binding ability of BPA and 4-OHT, but do not cause inactivity. It is evident that only Glu275 can elicit full activity, as long as the Arg316 residue is retained.

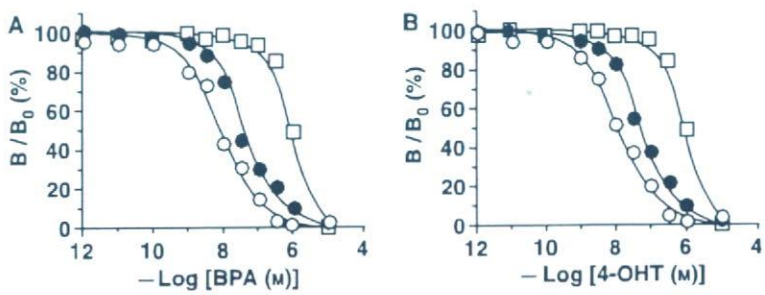

Fig. 5. Receptor competitive binding assays for the ERRγ and its mutants using [^{3}H]BPA. The assays were carried out to measure the ability to displace [^{3}H]BPA for wild-type ERRγ (○), (275*Ala*)-ERRγ with the Glu275 → Ala substitution (●), and (316*Ala*)-ERRγ with the Arg316 → Ala substitution (□). Chemicals used are BPA (A) and 4-OHT (B). The graphs show representative dose-dependent binding curves, which give the IC_{50} value closest to the mean IC_{50} from at least five independent assays. The IC_{50} values showed a between-experiment coefficient of variation of 4–9%. All the receptors used are the LBD of the human ERRγ and its mutant receptors.

The inactivity of (316*Leu*)-ERRγ and the extremely weak activity of (316*Ala*)-ERRγ (Tables 1 and 2) definitely reveal the importance of the basic Arg residue for receptor activation. Instead of Arg with the guanidino -NH-CH(=NH)NH_2 group, there is Lys with the amino group. Prepared (316*Lys*)-ERRγ was found to be considerably potent for binding [^{3}H]BPA (K_D = 22.5 nM) (Table 1). In the competitive binding assay using (316*Lys*)-ERRγ and [^{3}H]BPA, BPA was significantly active (IC_{50} = 37.1 nM) (Table 2). However, these activities are only approximately 25% that of the parent wild-type receptor ERRγ. Collectively, these results indicated that Arg316 is the most important structural element for the binding of BPA and 4-OHT to the binding pocket of ERRγ-LBD by hydrogen bonding.

Residual exchange between Glu275 and Arg316 keeps BPA in a binding pocket

It is now clear that Glu275 and Arg316 are necessary to hold BPA and 4-OHT in ERRγ, but with different degrees of involvement in the hydrogen bonding. The results clearly indicated the chief importance of phenol-hydroxyl↔Arg316 hydrogen bonding, whereas a corroborative role was indicated for the phenol-hydroxyl↔Glu275 hydrogen bonding. Given that the roles of these residues definitely confirm each other, the difference in their significance might be attributable to the importance and/or necessity of the receipt of the phenol-hydroxyl group, even by using an assisting group to facilitate the receptor function. No other amino acids would reward such an intrinsic role of a combination of 316Arg and 275Glu.

Thus, if we simply put these residues in opposite order, the resulting (*Arg*, *Glu*)-ERRγ double-mutant receptor would be exchangeable, but would have considerably lower affinity to BPA and 4-OHT. The mismatched proximity of Arg275 and Glu316 to the phenol-hydroxyl group of BPA and of 4-OHT would take place because an unchanged backbone structure is strongly suspected for α-helix-rich ERRγ-LBD. Indeed, these chemicals were found to bind to the (*Arg*, *Glu*)-ERRγ double-mutant receptor. However, as expected, they bound to the receptor approximately ten-fold more weakly than to the wild-type receptor (Tables 1 and 2).

Although Glu275 and Arg316 in ERRγ were found to be exchangeable for maintaining the interaction with BPA and 4-OHT (Table 2), their ability either to hold or have a role in retaining the phenol compounds in the resulting (*Arg*, *Glu*)-ERRγ receptor might be the same as that for the wild-type ERRγ. Further substitution of 275*Arg* and 316*Glu* with Ala resulted in a similar outcome: the chief role of phenol-hydroxyl↔275*Arg* hydrogen bonding and a corroborative role of the phenol-hydroxyl↔316*Glu* hydrogen bond. (*Ala*, *Glu*)-ERRγ mutant receptor with the 275*Arg* → Ala substitution was found to completely lack the binding capability for [^{3}H]BPA, whereas the Arg-containing (*Arg*, *Ala*)-ERRγ mutant receptor was still active (Table 1). It should be noted that (*Arg*, *Glu*)-ERRγ is almost equipotent with (*Arg*, *Ala*)-ERRγ (Table 1). This indicates that the corroborative role of the phenol-hydroxyl↔316*Glu* hydrogen bond is almost negligible. As a result, the wild-type ERRγ receptor appears to afford simultaneously an ideal space and the capability of arresting the phenol-hydroxyl groups by arranging the Glu and Arg residues at positions 275 and 316, respectively.

Evaluation of the basal constitutive activity of ERRγ mutant receptors

We examined the biological activity of BPA in the reporter gene assay in HeLa cells transiently cotransfected with an ERRγ receptor expression plasmid and an ERR response element (ERRE)-luciferase reporter plasmid. For reference estimations, the cells were treated with a vehicle solution to measure the basal constitutive activity of each receptor, by using exactly the same of amount of expression plasmid of the receptor. Furthermore, to normalize for transfection efficiency, we carried out simultaneously a SEAP assay [23], in which we cotransfected a second plasmid that constitutively expresses an activity that can be clearly differentiated from SEAP.

When we compared ERRγ mutant receptors with wild-type ERRγ, we found the constitutive activity levels differed considerably. As shown in Fig. 6A, the (275*Ala*)-ERRγ mutant receptor exhibited moderately elevated constitutive activity (42% of the basal activity of wild-type ERRγ). However, the (316*Ala*)-ERRγ mutant receptor with the Arg → Ala substitution exhibited considerably diminished constitutive activity (25%), and (*Ala*, *Ala*)-ERRγ became very weak (9%). These results clearly show that both Glu275 and Arg316, especially the latter residue, are important for constructing a high level of basal activity.

The wild-type ERRγ is fully activated spontaneously with no ligand. BPA (10^{-10} to 10^{-5} M) sustains this high level of ERRγ basal constitutive activity (Fig. 6B), as reported previously [12]. By contrast, BPA exhibited an extremely weak tendency to activate the mutant receptors of (275*Ala*)-ERRγ and (316*Ala*)-ERRγ in a

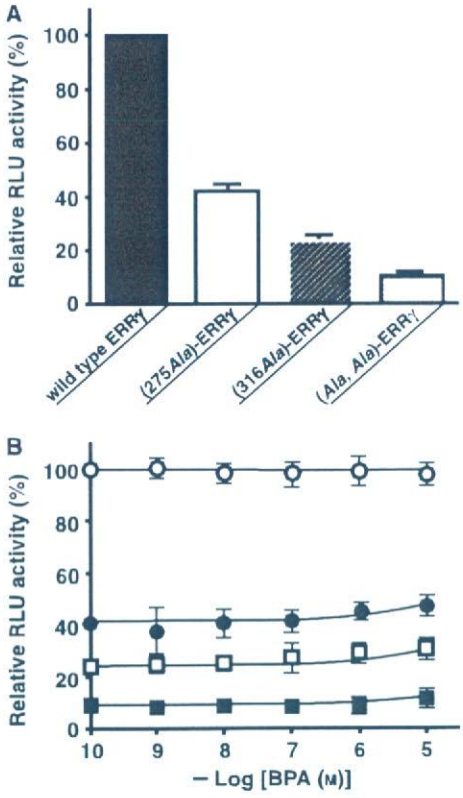

Fig. 6. Biological activity of the ERRγ and its site-directed mutant derivatives, by means of the luciferase-reporter gene assay. (A) The percentage relative potencies of a series of mutant receptors were measured against the basal constitutive activity of the wild-type ERRγ receptor (100%). An internal control that distinguishes the transcriptional level from variations in transfection efficiency was achieved by cotransfecting a second plasmid that constitutively expresses an activity that can be clearly differentiated from SEAP. (B) The effect of BPA on the basal constitutive activities of wild-type ERRγ (100%) and its mutant receptors. The graphs show the activity of wild-type ERRγ (○), (275*Ala*)-ERRγ (●), (316*Ala*)-ERRγ (□), and (*Ala, Ala*)-ERRγ (■) with 10^{-10} to 10^{-5} M BPA.

dose-dependent manner (Fig. 6B). For (275*Ala*)-ERRγ, 10 μM BPA increased the basal constitutive activity by 7%, reaching 49% of that of the wild-type ERRγ. For (316*Ala*)-ERRγ, 10 μM BPA also increased basal constitutive activity 7%, reaching 32% that of the wild-type ERRγ. This effect of BPA was found to be small (only approximately 3%) for (*Ala, Ala*)-ERRγ. These results clearly indicate that BPA functions to preserve the basal activity of ERRγ due to its strong binding, but that its binding to the mutant receptors is not sufficient to keep their conformation in a fully activated form. The Arg316 → Ala and Glu275 → Ala substitutions appear to damage intrinsically the activation conformation to a level that BPA is unable to rescue completely.

It was reported that 4-OHT deactivates ERRγ [12,24], diminishing the basal activity of ERRγ by up to 70–85% at a concentration of 10 μM (Fig. 7). BPA, on the other hand, showed no effect on the basal constitutive activity of ERRγ even at a concentration of 10 μM, completely preserving the high constitutive activity of ERRγ [12] (Figs 6 and 7). However, it should be noted that BPA reverses the inverse agonist activity of 4-OHT in a dose-dependent manner (Fig. 7). This effect of BPA has been acknowledged as an inverse antagonist activity on the constitutive activity of ERRγ [12]. Exactly the same receptor responses were observed for the (275*Ala*)-ERRγ mutant receptor (Fig. 7). It is noteworthy that the inverse agonist activity of 4-OHT and the inverse antagonist activity of BPA are observed for both (275*Ala*)-ERRγ and (316*Ala*)-ERRγ mutant receptors, and even for (*Ala, Ala*)-ERRγ.

Discussion

Differential capacity of Glu275 and Arg316 to interact with the ligand

In the present study, to inspect the structural elements of the ERRγ receptor in arresting BPA, we prepared 11 different analogue receptors with site-directed mutagenesis at positions 275 and 316. X-ray crystal structural analysis has suggested that the Glu275 and Arg316 residues each make a hydrogen bond with the phenol-hydroxyl group of BPA [20]. The present results clearly demonstrated that these residues are indeed involved in such hydrogen bonding interactions. Simultaneous mutation of these residues to Ala eliminated activity in binding to a BPA molecule, and individual mutations drastically reduced the activity. Because Ala lacks the characteristic side chains of Glu and Arg, the mutant receptors are devoid of the functional groups at the particular positions of 275 and 316. Thus, it becomes difficult for them to keep BPA in the ligand-binding pocket.

Interestingly, it became clear that Glu275 and Arg316 play roles in detaining BPA with different weights or levels of significance. The phenol-hydroxyl ↔Arg316 hydrogen bonding was found to play a major role, whereas the phenol-hydroxyl↔Glu275 hydrogen bonding plays a definite supporting role. In the saturation binding of [^{3}H]BPA, the extent of the decrease in the deactivation of the ERRγ receptor was much more drastic (by approximately 30-fold; Table 1) for the Arg316 → Ala substitution than that (approximately three-fold) for the Glu275 → Ala substitution,

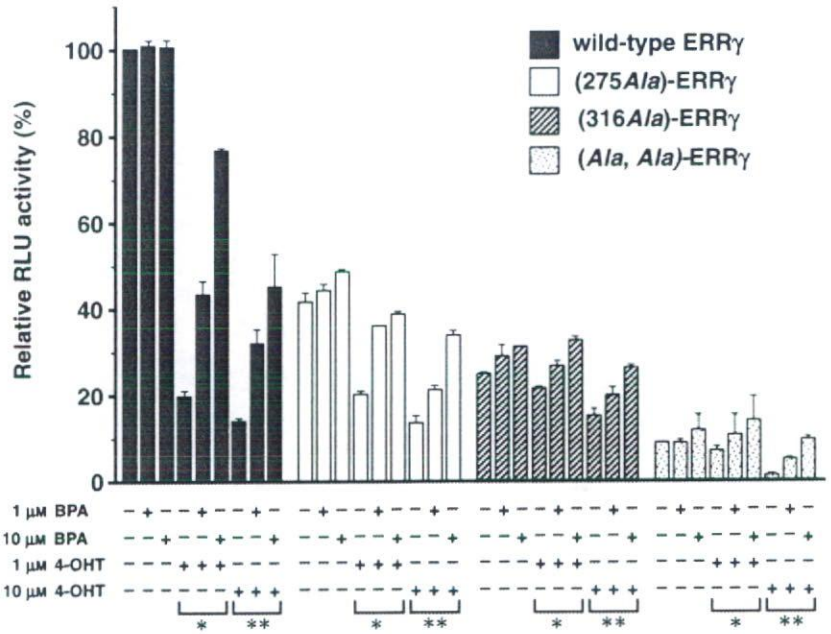

Fig. 7. Luciferase-reporter gene assays of BPA and 4-OHT for the ERRγ and its site-directed mutant derivatives. Assays were carried out to construct the concentration-dependent responses (1 and 10 μM) of BPA and 4-OHT in the luciferase-reporter gene assay. The basal constitutive activities of wild-type ERRγ (100%) and its mutant receptors were measured with no compounds. Normalization was achieved by simultaneous SEAP assays. The graphs show the basal constitutive activity, the activity of BPA (1 and 10 μM) for the basal constitutive activity, the inverse agonist activity of 4-OHT (1 and 10 μM) for the basal constitutive activity, and the inverse antagonist activity of BPA (1 and 10 μM) against the inverse agonist activity of 4-OHT (1 and 10 μM). The assay set marked with an asterisk shows the the inverse antagonist activity of BPA for 1 μM 4-OHT, and the other set marked by a double asterisk shows the the inverse antagonist activity of BPA for 10 μM 4-OHT. The receptors used are wild-type ERRγ, (275*Ala*)-ERRγ, (316*Ala*)-ERRγ, and (*Ala*, *Ala*)-ERRγ.

implying that Arg316 is much more important than Glu275 for [^{3}H]BPA binding.

It should be noted that the importance of the Arg-guanidino group was also demonstrated for the mutant receptor (*Arg*, *Glu*)-ERRγ, in which Arg and Glu are exchanged at the positions 275 and 316. (*Arg*, *Glu*)-ERRγ itself is still fairly potent for [^{3}H]BPA ($K_D \approx 60$ nM, approximately ten-fold larger than that of the parent ERRγ; Table 1). However, when the 275*Arg* → Ala substitution was given to this (*Arg*, *Glu*)-ERRγ mutant receptor, the resulting double-mutated receptor (*Ala*, *Glu*)-ERRγ became completely inactive for [^{3}H]BPA (Table 1). By contrast, another double-mutated receptor (*Arg*, *Ala*)-ERRγ, obtained by the 316*Glu* → Ala substitution, was found to be as active as the parent (*Arg*, *Glu*)-ERRγ (Table 1). The replacement of 316*Glu* with Ala had no effect on the binding ability of [^{3}H]BPA.

All these results clearly indicate the crucial role of Arg316 for the ERRγ receptor in ligand binding. This kind of structure–activity relationship between NRs and ligands has never been explored, and thus it is very important to seek an amino acid residue that is influential in, or definitive for, particular functions.

Evolutionary rationale for the major role of Arg316 in arresting the ligand

When the amino acid sequences of the LBD of all the NRs were aligned to that of ERRγ, it became noticeable that 26 receptors among the total 48 NRs [13] have Arg at the position corresponding to 316 (Fig. 8). In particular, all the members of Groups III, IV, and V NRs, consisting of nine, three, and two members, respectively, contain Arg at that particular position. There are seven Arg316-containing receptors in 19 Group I NRs and five in 12 Group II NRs. The fact that Arg316 is extremely highly conserved among NRs is remarkable because it constructs a part of the ligand-binding pocket inside each receptor. We reason that it must have been preserved in order to accept the similar structural elements of the ligands (e.g. the phenol-hydroxyl group) during the evolution of these diverse receptors.

On the other hand, Glu275 is conserved among only five NRs: ERs α and β, and ERRs α, β, and γ (Fig. 8). Although Glu possesses the carboxyl COOH group at the Cγ position, some other Arg316-containing NRs were found to have Gln at position 275. Instead of

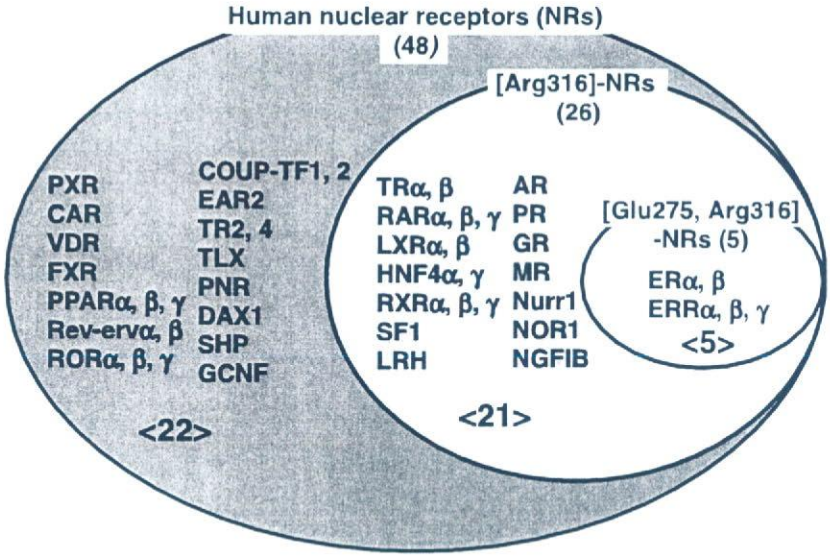

Fig. 8. Fractional grouping of the 48 human nuclear receptors according to residue variation at positions 316 and 275. Among 48 human nuclear receptors [13], the smallest is a group with five members whose nuclear receptors possess both Arg316 and Glu275, and the second group includes the 21 receptors containing Arg316.

COOH, Gln possesses the carboxyl amide $CONH_2$ group, which also retains both proton-donating and -accepting characters. However, as shown in the present study, Gln cannot necessarily replace the Glu275. It appears that (Glu275, Arg316)-containing NRs and (Gln275, Arg316)-containing NRs have different structural bases to receive each specific ligand.

Nine NRs contain the Gln275 and Arg316 residues simultaneously, and they belong to either Group II (five of 12) or Group III (four of nine) NRs. Other Arg316-containing NRs show a variety of amino acid residues at position 275: Ala ($n = 2$), Ser ($n = 5$), Thr ($n = 2$), and Cys ($n = 3$). When these residues including Gln are involved in the interaction with the ligand, they may be cooperative or collaborative with Arg316. All these details strongly suggest that Arg316 plays a principal role in selecting and binding the ligand for receptor activation. Of course, each individual NR should bind a specific ligand in a manner that differs from that by which other NRs bind their ligand, and thus the role of Arg316 must be different in some cases. Because the tasks played by Arg are varied and potent enough to cause the interaction with the ligand by means of electrostatic interaction, hydrogen bonding, and the so-called NH/π interaction, Arg316 may play the main role in arresting and keeping the ligand in the pocket.

Influence of residual mutation of ERRγ upon the basal constitutive activity

Compared to the high basal constitutive activity of the wild-type ERRγ receptor, the (275*Ala*)-ERRγ mutant receptor with the Glu275 → Ala substitution exhibited lessened, but still considerable basal activity (approximately 40% that of the wild-type) (Fig. 6). (275*Ala*)-ERRγ retains the Arg residue at position 316. However, mutant receptor Arg316 → Ala substitution showed very much weakened basal activity. (316*Ala*)-ERRγ exhibited basal constitutive activity, only approximately 20% that of the wild-type. Moreover (*Ala*, *Ala*)-ERRγ exhibited extremely weak basal activity. These data indicate that Arg316 is crucial in exhibiting biological activity as well as in ligand-binding.

In the case of the mutant receptor (275*Ala*)-ERRγ, with approximately 40% of the activity of wild-type ERRγ, 10 μM BPA only slightly enhanced activity (Figs 6 and 7). It appears to be difficult for BPA to completely occupy the ligand-binding pocket of (275*Ala*)-ERRγ. This is apparently because of the Glu275 → Ala substitution, and thus the slight increase in activity must be due to the ability of BPA to reconstruct an inactivated conformation into an activated one. BPA in the ligand-binding pocket of (275*Ala*)-ERRγ should hold H12 for the position in the active conformation. It is evident that such an effect of BPA is only partial, presumably because the binding of BPA to (275*Ala*)-ERRγ is not so stable. As for (316*Ala*)-ERRγ, this kind of reconstruction appears much more difficult.

For the inverse antagonist activity of BPA, the presence of an inverse agonist and its binding to the receptor is indispensable. 4-OHT exhibited reasonable receptor binding affinity for both the (275*Ala*)-ERRγ and (316*Ala*)-ERRγ receptors (Table 2) and, in the reporter gene assay, it showed definite inverse agonist activity for these mutant receptors, and even for

(*Ala*, *Ala*)-ERRγ (Fig. 7). BPA was found to clearly reverse the inverse agonist activity of 4-OHT in the wild-type ERRγ receptor and the mutant receptors, indicating that BPA displaces 4-OHT to convert to the activation conformation.

Conclusion

The present results reveal that ERRγ has residues (Gly275 and Arg316) to capture or arrest phenol compounds. Their individual substitutions revealed degrees of difference in activity reduction, indicating the major importance of phenol-hydroxyl↔Arg316 hydrogen bonding and the supportive role of phenol-hydroxyl↔Glu275 hydrogen bonding. The data obtained with characteristic mutations suggested that these hydrogen bonds are conducive to the recruitment of phenol compounds by ERRγ. The ERRγ receptor forms an appropriate structure presumably to adopt endogenous BPA-like ligand(s) that have yet to be identified.

Experimental procedures

Chemicals

BPA was purchased from Tokyo Kasei Kogyo Co., Ltd. (Tokyo, Japan). 4-OHT was obtained from Sigma-Aldrich Inc. (St Louis, MO, USA). [^{3}H]BPA (5 Ci·mmol^{-1}) was obtained from Moravek Biochemicals (Brea, CA, USA).

Plasmid construction and site-directed mutagenesis

A cDNA fragment encoding wild-type ERRγ-LBD (residues 222–458) was generated by PCR with specific primers using the human kidney cDNA library (Clontech Laboratories, Mountain View, CA, USA) and cloned into the vector pGEX-6p-1 (Amersham Biosciences, Piscataway, NJ, USA) at the *Eco*RI and *Xho*I sites. Full-length wild-type ERRγ was also amplified from the human kidney cDNA library by PCR and cloned into pcDNA3.1(+) (Invitrogen, Carlsbad, CA, USA) also at the *Eco*RI and *Xho*I sites. The resulting plasmids were designated as pGEX-ERRγ-LBD and pcDNA3.1-ERRγ-Full, respectively.

ERRγ mutants were generated using *PfuTurbo*® DNA Polymerase (Stratagene, La Jolla, CA, USA) according to the manufacturer's instructions using pGEX-ERRγ-LBD or pcDNA3.1-ERRγ-Full as a template. The mutations were introduced by PCR mutagenesis in a two-step reaction [21]. The primers used were: 5′-ACTTGGCCGACCGA*xxx*T TGGTGGTTA-3′ (*xxx* = *gcg* for Glu275Ala, *cgg* for Glu275Arg, *gac* for Glu275Asp, and *ctg* for Glu275Leu); 5′-TCCTTGGTGTCGTATAC*xxx*TCTCTTTCA-3′ (*xxx* = *gcg* for Arg316 → Ala, *aag* for Arg316 → Lys, *ctg* for Arg316 → Leu, and *gag* for Arg316 → Glu). Each mutant LBD or full-length ERRγ was amplified and cloned into the vector pGEX-6p-1 or pcDNA3.1(+) at the *Eco*RI and *Xho*I sites. All PCR products were verified for their accuracy in the sequences. As an ERRE-luciferase construct, 3 × ERRE/pGL3 was used as described previously [12].

ERRγ-LBD protein expression

Two GST-fused receptor proteins (the wild-type and mutant GST-ERRγ-LBD) were expressed in *E. coli* BL21 as described previously [12]. The mixture was centrifuged, and the resulting pellet was sonicated in 2–20 mL of buffer (50 mM Tris/HCl, pH 8.0, 50 mM NaCl, 1 mM EDTA, and 1 mM dithiothreitol). The receptor protein was purified by using an affinity column of Glutathione-Sepharose 4B (GE Healthcare BioSciences Co., Piscataway, NJ, USA). After incubation for 1 h at 4 °C, the column was washed three times with phosphate buffered saline (NaCl/P$_i$) containing 0.2% (v/v) Triton X-100 and once with the same sonication buffer described above. Fusion protein was eluted with 1 M Tris/HCl (pH 8.0) containing 20 mM reduced glutathione, which was removed by gel filtration on a column of Sephadex G-10 (15 × 100 mm, GE Healthcare) equilibrated with 50 mM Tris/HCl (pH 8.0). The purity was confirmed by SDS/PAGE using 12.5% polyacrylamide gel. The protein concentration was determined by the Bradford method [25].

Radioligand binding assays

Saturation binding

A saturation binding assay was conducted essentially as reported [26], by using [^{3}H]BPA. The reaction mixture was incubated overnight at 4 °C with the receptor proteins (GST-fused wild-type ERRγ-LBD or its mutants) in 100 μL binding buffer (10 mM Hepes, pH 7.5, 50 mM NaCl, 2 mM $MgCl_2$, 1 mM EDTA, 2 mM CHAPS, and 2 mg·mL^{-1} γ-globulins). The assay was performed with or without the addition of unlabeled BPA or 4-OHT (final concentration of 1 × 10^{-5} M) to quantify the specific and nonspecific binding. After incubation with 100 μL of 1% dextran-coated charcoal (Sigma) in NaCl/P$_i$ (pH 7.4) for 10 min at 4 °C, free radioligand was removed by the direct vacuum filtration method using a 96-well filtration plate (Millipore, Bedford, MA, USA) for the B/F separation. The specific binding of [^{3}H]BPA was calculated by subtracting the nonspecific binding from the total binding, and the results were examined by Scatchard plot analysis. The assay was carried out at least in triplicate.

Competitive binding

Competitive binding assays were performed in the presence of GST-fused wild-type ERRγ-LBD or its mutants at the most appropriate concentration of each. Reaction mixtures were incubated with [^{3}H]BPA (5 nM in final) at 4 °C overnight, and free radioligand was removed by the method described above after incubation with 100 μL of 1% dextran-coated charcoal in NaCl/P_i (pH 7.4) for 10 min at 4 °C. To estimate the binding affinity, the IC_{50} values were calculated from the dose–response curves evaluated by the nonlinear analysis program ALLFIT [27]. Each assay was performed in duplicate and repeated at least three times.

Cell culture and transient transfection assays

HeLa cells were maintained in Eagle's modified Eagle medium (EMEM) (Nissui, Tokyo, Japan) in the presence of 10% (v/v) fetal bovine serum at 37 °C. HeLa cells were seeded at 5×10^5 cells/dish (6 cm in diameter) for 24 h and then transfected with a mixture of 3 μg of luciferase reporter gene (pGL3/3xERRE), 1 μg of the expression plasmid of wild-type ERRγ or its mutant [pcDNA3.1(+)/ERRγ-WT or mutations] and, as an internal control, 10 ng of pSEAP-control plasmid by Plus reagent (10 μL·mL^{-1}; Invitrogen) and Lipofectamine (15 μL·mL^{-1}), according to the manufacturer's protocol. Approximately 24 h after transfection, cells were harvested and plated into 96-well plates at a concentration of 5×10^4 cells/well. The cells were then treated with varying doses of chemicals diluted with 1% BSA/NaCl/P_i (v/v).

After 24 h, luciferase activity was measured by using Luciferase assay reagent (Promega, Madison, WI, USA) according to the manufacturer's instructions. SEAP activity was assayed by using Great EscAPe™ SEAP assay reagent (Clontech Laboratories) according to the Fluorescent SEAP Assay protocol. Light emission was measured on a microplate reader Wallac 1420 ARVOsx (Perkin Elmer, Turku, Finland). Cells treated with 1% BSA/NaCl/P_i were used as a vehicle control. Values were computed as fold inductions after normalization to SEAP activities. Each assay was performed in duplicate and repeated at least three times.

Acknowledgements

We thank Professor Ian A. Meinertzhagen, Dalhousie University, Canada, for reading the manuscript. This study was supported in part by Health and Labour Sciences Research Grants for Research on Risk of Chemical Substances from the Ministry of Health, Labor and Welfare of Japan. This work was also supported in part by grants-in-aid from the Ministry of Education, Science, Sports and Culture in Japan to YS.

References

1 Dodds EC & Lawson W (1938) Molecular structure in relation to oestrogenic activity. Compounds without a phenanthrene nucleus. *Proc R Soc Lond B Biol Sci* **125**, 222–232.

2 Krishnan AV, Stathis P, Permuth SF, Tokes L & Feldman D (1993) Bisphenol-A: an estrogenic substance is released from polycarbonate flasks during autoclaving. *Endocrinology* **132**, 2279–2286.

3 Olea N, Pulgar R, Perez P, Olea-Serrano F, Rivas A, Novillo-Fertrell A, Pedraza V, Soto AM & Sonnenschein C (1996) Estrogenicity of resin-based composites and sealants used in dentistry. *Environ Health Perspect* **104**, 298–305.

4 Sohoni P & Sumpter JP (1998) Several environmental oestrogens are also anti-androgens. *J Endocrinol* **158**, 327–339.

5 Xu LC, Sun H, Chen JF, Bian Q, Qian J, Song L & Wang XR (2005) Evaluation of androgen receptor transcriptional activities of bisphenol A, octylphenol and nonylphenol in vitro. *Toxicology* **216**, 197–203.

6 vom Saal FS, Cooke PS, Buchanan DL, Palanza P, Thayer KA, Nagel SC, Parmigiani S & Welshons WV (1998) A physiologically based approach to the study of bisphenol A and other estrogenic chemicals on the size of reproductive organs, daily sperm production, and behavior. *Toxicol Ind Health* **14**, 239–260.

7 Kubo K, Arai O, Omura M, Watanabe R, Ogata R & Aou S (2003) Low dose effects of bisphenol A on sexual differentiation of the brain and behavior in rats. *Neurosci Res* **45**, 345–356.

8 vom Saal FS & Hughes C (2005) An extensive new literature concerning low-dose effects of bisphenol A shows the need for a new risk assessment. *Environ Health Perspect* **113**, 926–933.

9 National Toxicology Program (NTP) (2001) US Department of Health and Human Services, National Institute of Environmental Health Sciences, National Toxicology Program's Report of the Endocrine Disruptors Low-Dose Peer Review. Available at http://ntp-server.inehs.nih.gov./htdcs/liason/LowDoseWebPage.html.

10 Safe SH, Pallaroni L, Yoon K, Gaido K, Ross S & McDonnell D (2002) Problems for risk assessment of endocrine-active estrogenic compounds. *Environ Health Perspect* **110**, 925–929.

11 Gray GM, Cohen JT, Cunha G, Hughes C, McConnell EE, Rhomberg L, Sipes IG & Mattison D (2004) Weight of the evidence evaluation of low dose reproductive and developmental effects of bisphenol A. *Hum Ecol Risk Assess* **10**, 875–921.

12 Takayanagi S, Tokunaga T, Liu X, Okada H, Matsushima A & Shimohigashi Y (2006) Endocrine disruptor bisphenol A strongly binds to human estrogen-related

receptor γ (ERRγ) with high constitutive activity. *Toxicol Lett* **167**, 95–105.

13 Robinson-Rechavi M, Carpentier AS, Duffraisse M & Laudet V (2001) How many nuclear hormone receptors are there in the human genome? *Trends Genet* **17**, 554–556.

14 Giguere V (2002) To ERR in the estrogen pathway. *Trends Endocrinol Metab* **13**, 220–225.

15 Horard B & Vanacker JM (2003) Estrogen receptor-related receptors: orphan receptors desperately seeking a ligand. *J Mol Endocrinol* **31**, 349–357.

16 Eudy JD, Yao S, Weston MD, Ma-Edmonds M, Talmadge CB, Cheng JJ, Kimberling WJ & Sumegi J (1998) Isolation of a gene encoding a novel member of the nuclear receptor superfamily from the critical region of Usher syndrome type IIa at 1q41. *Genomics* **50**, 382–384.

17 Hong H, Yang L & Stallcup MR (1999) Hormone-independent transcriptional activation and coactivator binding by novel orphan nuclear receptor ERR3. *J Biol Chem* **274**, 22618–22626.

18 Heard DJ, Norby PL, Holloway J & Vissing H (2000) Human ERRgamma, a third member of the estrogen receptor-related receptor (ERR) subfamily of orphan nuclear receptors: tissue-specific isoforms are expressed during development and in the adult. *Mol Endocrinol* **14**, 382–392.

19 Greschik H, Wurtz JM, Sanglier S, Bourguet W, van Dorsselaer A, Moras D & Renaud JP (2002) Structural and functional evidence for ligand-independent transcriptional 1 evidence for ligand-independent transcriptional activation by the estrogen-related receptor 3. *Mol Cell* **9**, 303–313.

20 Matsushima A, Kakuta Y, Teramoto T, Koshiba T, Liu X, Okada H, Tokunaga T, Kawabata S, Kimura M & Shimohigashi Y (2007) Structural evidence for endocrine disruptor bisphenol A binding to human nuclear receptor ERRγ. *J Biochem* **142**, 517–524.

21 Nelson RM & Long GL (1989) A general method of site-specific mutagenesis using a modification of the *Thermus aquaticus* polymerase chain reaction. *Anal Biochem* **180**, 47–51.

22 Greschik H, Flaig R, Renaud JP & Moras D (2004) Structural basis for the deactivation of the estrogen-related receptor gamma by diethylstilbestrol or 4-hydroxytamoxifen and determinants of selectivity. *J Biol Chem* **279**, 33639–33646.

23 Sambrook J & Russell DW (2001) *Molecular Cloning: A Laboratory Manual*, 3rd edn. Cold Springs Harbor Laboratory Press, Cold Spring Harbor, NY.

24 Coward P, Lee D, Hull MV & Lehmann JM (2001) 4-Hydroxytamoxifen binds to and deactivates the estrogen-related receptor gamma. *Proc Natl Acad Sci USA* **98**, 8880–8884.

25 Bradford MM (1976) A rapid and sensitive method for the quantitation of microgram quantities of protein utilizing the principle of protein-dye binding. *Anal Biochem* **72**, 248–254.

26 Nakai M, Tabira Y, Asai D, Yakabe Y, Shimyozu T, Noguchi M, Takatsuki M & Shimohigashi Y (1999) Binding characteristics of dialkyl phthalates for the estrogen receptor. *Biochem Biophys Res Commun* **254**, 311–314.

27 DeLean A, Munson PJ & Rodbard D (1978) Simultaneous analysis of families of sigmoidal curves: application to bioassay, radioligand assay, and physiological dose–response curves. *Am J Physiol* **235**, E97–E102.

J. Biochem. **141,** 867–877 (2007)
doi:10.1093/jb/mvm094

Double-labelled *in situ* Hybridization Reveals the Lack of Co-localization of mRNAs for the Circadian Neuropeptide PDF and FMRFamide in Brains of the Flies *Musca domestica* and *Drosophila melanogaster*

Ayami Matsushima[1], Katsuhiro Takano[2], Taichi Yoshida[1], Yukimasa Takeda[1], Satoru Yokotani[1], Yasuyuki Shimohigashi[1,*] and Miki Shimohigashi[2]

[1]Laboratory of Structure-Function Biochemistry, Department of Chemistry, Faculty and Graduate School of Sciences, Kyushu University, Fukuoka 812-8581, Japan; and [2]Division of Biology, Faculty of Science, Fukuoka University, Fukuoka 814-0180, Japan

Received January 9, 2007; accepted March 31, 2007; published online April 10, 2007

Many lines of evidence have suggested that neuropeptides other than pigment-dispersing factor (PDF) are involved in regulating insect circadian rhythms, and FMRFamide-related peptides are additional candidates acting as such neuromodulators. Double-immunolabelling in insect brains with anti-crustacean β-PDH and anti-FMRFamide antibodies had previously suggested that insect PDF and FMRFamide-like peptides may coexist in the same cells. However, it is critical for this kind of comparative investigations to use antibodies of proven specificity, to eliminate the possibility of both reciprocal cross-reactivity and the detection of unknown peptides. In the present study, we achieved the cDNA cloning of an *fmrf* mRNA from the housefly *Musca domestica*, for which co-localization of FMRFamide and PDF peptides was previously suggested. In order to examine the possible co-expression of this gene with the *pdf* gene, we carried out double-labelled *in situ* hybridization for simultaneous detection of both *pdf* and *fmrf* mRNAs in housefly, *Musca* brains. The results clearly indicated that they occur in distinctly different cells. This was also proven for the fruit fly *Drosophila melanogaster* by similar double-labelled *in situ* hybridization. The results thus revealed no reason to evoke the physiological release of FMRFamide and PDF peptides from the same neurons.

Key words: circadian rhythm, double-labelled *in situ* hybridization, FMRFamides, neuropeptides, pigment-dispersing factor (PDF).

Abbreviations: AAP, Abridged Anchor Primer; AP, alkaline phosphatase; AUAP, Abridged Universal Anchor Primer; BCIP, 5-bromo-4-chloro-3-indolylphosphate; DCV, dense core vesicle; DIG, digoxigenin; FaRPs, FMRFamide-related peptides; FITC, fluorescein isothiocyanate; FMRFamide, the one-letter amino acid code denotes H–Phe–Met–Arg–Phe–NH_2; HRP, horseradish peroxidase; NBT, 4-nitro-blue tetrazolium chloride; NTMT, a solution containing 100 mM NaCl, 100 mM Tris–HCl (pH 9.5), 50 mM MgCl2 and 1% Tween 20; PBS, phosphate buffered saline; PBST, PBS containing 0.1% Tween 20; PDF, pigment-dispersing factor; PDH, pigment-dispersing hormone; RACE, rapid amplification of cDNA ends; RT-PCR, reverse transcription PCR; TBS, Tris-buffered saline; TBST, TBS containing 1% Tween 20.

FMRFamide (H–Phe–Met–Arg–Phe–NH_2) is a neuropeptide originally isolated from the mollusk *Macrocallista nimbosa* and identified by monitoring its cardioexcitatory activity on the clam heart (*1*). Peptides containing C-terminal FMRFamide or a related sequence are members of a large family of structurally related peptides found in both invertebrate and vertebrate species. In insects, these peptides are called FMRFamide-related peptides (FaRPs) and three major families have been reported to date, including FMRFamides, sulfakinins (*2*) and myosuppressins (*3, 4*). However, little is known about their physiological functions.

Another insect amide peptide, pigment-dispersing factor (PDF), was first found in brains of the grasshopper and its melanophore pigment-dispersing activity monitored in crabs (*5*). Insect PDF is composed of 18 amino acids and involved in the regulation of circadian rhythms as an output neuromodulator (*6–14*). Its involvement in circadian rhythm was shown by the mutant fruit fly *Drosophila melanogaster* designated pdf^{01}. pdf^{01} was found to have a nonsense mutation at the residue 21 of prepro-PDF, converting a Tyr (TAC) to a stop codon (TAA). This mutant shows abnormal behaviour, the evening activity peak being advanced by approximately 1 h (*11*). The result revealed the substantial importance of *pdf* in circadian system. In order to elucidate the molecular mechanism of PDF peptide in the regulation of circadian rhythms, we have cloned *pdf*

*To whom correspondence should be addressed. Tel/Fax: +81-92-642-2584, E-mail: shimoscc@mbox.nc.kyushu-u.ac.jp

The nucleotide sequence datum reported in this article has been submitted to the DDB/EMBL/GenBank Data libraries under accession number AB214648.

mRNAs from several insects and clarified the existence of four different types of precursor proteins (*15–19*).

In recent years, there have also been several reports suggesting the involvement of neuropeptides other than PDF in the circadian regulatory system, and FMRFamide peptides have been proposed as candidates for such neuromodulators. Microinjection of FMRFamide peptides into the brains of houseflies, for example, confirmed a strong interrelation between this neuropeptide and circadian rhythms in the visual system (*20*). Double-immunolabelling in insect brains using anti-crustacean β-PDH and anti-FMRFamide antibody had suggested moreover that insect PDF and FMRFamide-like peptides may co-exist in the same cells in several different insect species (*20–23*). However, immunocytochemical investigations crucially require the use of highly specific antibodies against each peptide in order to avoid possible cross-reactivity to unknown peptides.

As a check, multiple-labelling *in situ* hybridization techniques can provide sensitive cytochemical information about more than two different mRNA genes in the same preparation. This method requires the precise nucleotide sequence of a target mRNA in the preparation of cRNA probes. The recent cDNA cloning and *in situ* hybridization of *pdf* mRNA of the house fly *Musca domestica* (*17*), provided an excellent opportunity to examine the co-localization of *pdf* with *fmrf* mRNA in the *Musca* brain. *Musca* has a brain size bigger than that of the fruit fly *Drosophila* and this is definitely advantageous to identify the mRNA-expressing cells as a prior experiment to the analysis for *Drosophila* brain. Thus, in the present study we first carried out molecular cloning of *Musca fmrf* mRNA.

For insect FMRFamide-related peptides, available cloning data have hitherto been limited to two different fruit fly species, *D. melanogaster* and *D. virilis*. The *D. melanogaster fmrf* gene was identified by screening the genomic library using *fmrf* cDNA sequence data from the marine mollusk *Aplysia californica* (*24*) and eventually found to encode 13 copies of 8 different FaRPs, five copies of which are exactly identical (*25*). The *fmrf* gene of *D. virilis* was also cloned by screening the genomic library using the *D. melanogaster* genome fragment lying 5′ upstream of the *fmrf* mRNA start site (*26*). This *fmrf* gene encodes 10 different FaRPs, six of which are different from *D. melanogaster* FaRPs. Although such a low sequence similarity makes the search for *fmrf* genes in insects very difficult, based on this sequence information we planned to clone the housefly *fmrf* gene. Here we describe the results of cDNA cloning of the *Musca fmrf* gene and double-labelled *in situ* hybridization of both *fmrf* and *pdf* mRNAs.

MATERIALS AND METHODS

Animals—The housefly *Musca domestica* was purchased from Sumika Technoservice Co. (Takarazuka). All flies were maintained at 25°C under a day:night cycle of L12:D12. To collect brain samples for cDNA cloning, the flies were dissected under a microscope and their brains were immediately frozen in liquid nitrogen. Dissected thoracic ganglia of males and females were stored at −80°C until use. For *in situ* hybridization, 5-day-old female houseflies were used.

3′ RACE for Identification of 3′ End Coding Musca fmrf cDNA—The cDNA cloning of the *Musca fmrf* gene was carried out by the 3′ RACE method (*27*). mRNAs were extracted from the thoracic ganglia dissected from about 30 flies using a QuickPrep® *Micro* mRNA Purification Kit (Amersham Biosciences, Piscataway, NJ, USA) according to the Manufacturer's instructions. The mRNAs (300 ng) were reverse-transcribed by Super Script™ II reverse transcriptase (Invitrogen, Carlsbad, CA, USA) using $d(T)_{17}$-adapter primer (5′-GGCCACGCGTCGACTAGTAC-T_{17}-3′) at 42°C, as previously described (*16*). The resulting cDNAs were subjected to the polymerase chain reaction (PCR) using adaptor primer (5′-GGCCACGCGTCGACTAGTAC-3′) and degenerated primers PKQDFMRFG-F (5′-CCIHVI CARGAYTTYATGMGITT-3′), QDFMRFGR-F (5′-CARG AYTTYATGMGITTYGGIMG-3′) or DNFMRFGR-F (5′-GAYAAYTTYATGMGITTYGGIMG-3′). In these primers, the letters H, V, M, R and Y denote the nucleotides (not G), (not T), (A or C), (A or G) and (C or T), respectively. The primer was designed based on amino acid sequence homology between the FaRP peptide sequences for *D. melanogaster* and *Calliphora vomitoria* (*28*). PCR was performed using AccuPrime™ *Taq* DNA polymerase (Invitrogen) with a slight modification for touch-down PCR condition (*29*): *i.e.* the reaction condition used, 3 min at 94°C followed by 3 cycles of 94°C for 30 s, 68°C for 30 s, 72°C for 60 s, 3 cycles of 94°C for 30 s, 65°C for 30 s, 72°C for 60 s, 3 cycles of 94°C for 30 s, 63°C for 30 s, 72°C for 60 s, 3 cycles of 94°C for 30 s, 60°C for 30 s, 72°C for 60 s, 3 cycles of 94°C for 30 s, 58°C for 30 s, 72°C for 60 s, 25 cycles of 94°C for 30 s, 56°C for 30 s, 72°C for 60 s and a final extension for 7 min at 72°C. The PCR products were subcloned into pBluescript II SK+ and the sequence was analysed by a Thermo Sequenase Cy5.5 dye terminator cycle sequencing kit (Amersham Biosciences).

On the basis of the *Musca fmrf* sequence so obtained, gene-specific primers were newly designed and 3′ RACE was performed for a second time. The primers used were MuscaFMRF-F1 (5′-TGGCCGTAGTCCAGGAAGCCAA-3′ corresponding to the nucleotide sequence 1008–1029 in Fig. 1) and MuscaFMRF-F2 (5′-GCATCGGGTGGACA AGACTTCAT-3′ corresponding to the nucleotide sequence 1159–1181 in Fig. 1). The sequence analysed was confirmed by sequencing several other clones simultaneously.

5′ RACE for Identification of 5′ End Encoding Musca fmrf cDNA—To amplify the 5′ end of the *M. domestica fmrf* (denoted hereafter as *Musca fmrf*) cDNA, 5′ RACE (*26*) using the 5′ RACE System for Rapid amplification of cDNA ends Version 2.0 (Invitrogen) was performed according to the Manufacturer's protocol with some modifications. First-strand cDNA was synthesized from an mRNA by Super Script™ II reverse transcriptase (Invitrogen) with a *Musca fmrf*-specific antisense primer MuscaFMRF-R3 (5′-AAGCTCATGTTTATCGAAT-3′, corresponding to the nucleotide sequence 1485–1503 in Fig. 1) at 42°C. The product was digested by RNase H/T_1 to remove the original mRNA template.

```
   1 ACACAGACKTTCCAACGCTTCACCACAGTCAACAAGTGTCGTCATTCCSGGATATCACCACAT    63
  64 TGCCGGATCTTGTGTTGATTGAATTATTCTTGTAACGGATTTTTCACTTAATATTCAGAAAAA   126
 127 AAGTAATATCGGACTGCAAAATATTTGTGCAAAAATTGAAAGTGTTTTGTTTTTGAAAATAAA   189

 190 CTTTATTTAATTTTTGATATAACCATGGTGGCACCCCTACTTGTATTTTTGTTTTCGCTACAA   252
   1                             M  V  A  P  L  L  V  F  L  F  S  L  Q    13

 253 CTGTGTCACACCACATCGTGGGCCTATGTTGGGGGGAATTCTTTGAACTCCAATTCGCTACAT   315
  14  L  C  H  T  T  S  W  A  Y  V  G  G  N  S  L  N  S  N  S  L  H    34

 316 GCTTCTTATTCAGAATTCCCGGCCGGAACTTCGAATGAAGTGCCCGAAGATGCAGCAAATGGT   378
  35  A  S  Y  S  E  F  P  A  G  T  S  N  E  V  P  E  D  A  A  N  G    55

 379 CAAGATGACAATGATGACAGCCAACTGACAGAACCGAATGACAACAACGCCCCCTTGGTACAG   441
  56  Q  D  D  N  D  D  S  Q  L  T  E  P  N  D  N  N  A  P  L  V  Q    76

 442 AGTATAGATGATGAAACTGAAATGCAATTTCCCAAACCTATACAATGGGTCAGCATCGATCAT   504
  77  S  I  D  D  E  T  E  M  Q  F  P  K  P  I  Q  W  V  S  I  D  H    97

 505 TTACGCAATTCCATTATTTTGAGGTTTCAAAATCCCACCCCCAAGATTCTCAATAAACTTGAT   567
  98  L  R  N  S  I  I  L  R  F  Q  N  P  T  P  K  I  L  N  K  L  D   118

 568 CCCGAAGAAATGAAAAGATTGCGATCGCTGCAGGAGAATGCAATGCGCTGGGGAAAGCGATCA   630
 119  P  E  E  M  K  R  L  R  S  L  Q  E  N  A  M  R  W  G  K  R  S   139

 631 TACGAGAGTTATCCCTTGAATCGAAATGGTCTGGCCGACAAGAGCTCAGTGGGTCGCATGGGC   693
 140  Y  E  S  Y  P  L  N  R  N  G  L  A  D  K  S  S  V  G  R  M  G   160

 694 TTTTTGAGTAATCATCAAGTTATACGAGATTCCCGCGGTGATAATTTCATGCGCTTTGGCCGT   756
 161  F  L  S  N  H  Q  V  I  R  D  S  R  G  D  N  F  M  R  F  G  R   181

 757 TCGGTGGGTGGCAGTGGTGGTAATGATGATAATTTTATGCGTTTTGGTCGTGCATCGGGAAGC   819
 182  S  V  G  G  S  G  G  N  D  D  N  F  M  R  F  G  R  A  S  G  S   202

 820 AGTGATTTTATGCGTTTTGGTCGAGCGGGTCAGGATAATTTTATGCGCTTCGGTAGAGCGGCC   882
 203  S  D  F  M  R  F  G  R  A  G  Q  D  N  F  M  R  F  G  R  A  A   223

 883 GGACAAGACTTCATGCGTTTTGGTCGTGGTTCAGGACAAGATTTTATGCGATTTGGCCGATCA   945
 224  G  Q  D  F  M  R  F  G  R  G  S  G  Q  D  F  M  R  F  G  R  S   244

 946 CCAGGAAGTCAAGATTTCATGAGATTTGGTCGCAATCCAGGTTCGCAAGATTTTATGCGATTT  1008
 245  P  G  S  Q  D  F  M  R  F  G  R  N  P  G  S  Q  D  F  M  R  F   265

1009 GGCCGTAGTCCAGGAAGCCAAGATTTTATGCGTTTCGGCCGCAATCCAGGAAGCCAAGATTTT  1071
 266  G  R  S  P  G  S  Q  D  F  M  R  F  G  R  N  P  G  S  Q  D  F   286

1072 ATGAGATTTGGTCGCAATCCAGGATCCCAAGATTTTATGAGATTTGGTCGCAATCCAGGATCC  1134
 287  M  R  F  G  R  N  P  G  S  Q  D  F  M  R  F  G  R  N  P  G  S   307

1135 CAAGATTTCATGAGATTTGGTCGGGCATCGGGTGGACAAGACTTCATGAGATTTGGTCGAGCC  1197
 308  Q  D  F  M  R  F  G  R  A  S  G  G  Q  D  F  M  R  F  G  R  A   328

1198 CCCTCTGGCCAGGACTTTATGCGTTTCGGTAGACCCGATAATTTTATGCGCTTTGGTCGAACT  1260
 329  P  S  G  Q  D  F  M  R  F  G  R  P  D  N  F  M  R  F  G  R  T   349

1261 CCCGCACAATCAAGCGACTTTATGCGTTTCGGCAGAACCCCCACCCAATCCAGTGATTTCATG  1323
 350  P  A  Q  S  S  D  F  M  R  F  G  R  T  P  T  Q  S  S  D  F  M   370

1324 CGCTTTGGTAAAAGTCTAGATAAATCGGAAAATAAAACATCTGATCTACAAAAATAACAACAA  1386
 371  R  F  G  K  S  L  D  K  S  E  N  K  T  S  D  L  Q  K  *          388

1387 ATGGGAAAGAATGAACTTAAACAAGCCGTAAAACTTATACATGAAGCCGATAAAAATTCTGAA  1449
1450 AATGGTAACCCTGTCGATAAGGCCATTAAAGCTTTATTCGATAAACATGAGCTTGATGATCAC  1512
1513 AGCGTCGATAACATCGATGACAATCATGCGGCCGATCTTACACCACATGAAAACAATTCCGAT  1575
1576 GAACAAAATGCCGATTTGGATTACTTTCTCAACATGAAAATGACAAATTAATGGGAAAAAATC  1638
1639 AC(a)n
```

Fig. 1. **Nucleotide and deduced amino acid sequences of *Musca* FMRFamide.** A full-length cDNA clone comprises 1640 bp encoding a precursor protein of 388 amino acid residues. The FMRF structures, Phe–Met–Arg–Phe, are underlined, and the dibasic KR sites and monobasic sites GR and GK are double-underlined.

A homopolymeric tail poly(C) was elongated by using terminal deoxynucleotidyl transferase and a substrate dCTP. The resulting tailed cDNA was amplified by the Abridged Anchor Primer AAP (5′-GGCCACGCGTCG ACTAGTACGGGIIGGGIIGGGIIG-3′ provided by the kit, Life Tech.) and a *Musca fmrf* gene-specific antisense primer MuscaFMRF-R2 (5′-GGCCTTATCGACAGGGT TACCATTT-3′, corresponding to the nucleotide sequence 1449–1473 in Fig. 1) under the conditions essentially as for 3′ RACE. The PCR product was further amplified with Abridged Universal Anchor Primer (AUAP) (5′-GGC CACGCGTCGACTAGTAC-3′, Invitrogen) and *Musca fmrf* gene-specific antisense nested primer MuscaFM RF-R1 (5′-CTTCATGTATAAGTTTTACGGCTTGTT-3′ corresponding to the nucleotide sequence 1406–1432 in Fig. 1). The respective PCR and sequence analyses were carried out as described earlier, and the sequence analysed was confirmed by sequencing several different clones simultaneously.

In order to obtain the authentic full-length 5′ end, further 5′ RACE was performed by the procedure described earlier. One modification was to increase the temperature in a reverse transcription reaction by using newly designed primers. First-strand cDNA was prepared from mRNA with MuscaFMRF-R2 at 55°C, about 10°C higher than that in the previous run. The PCR amplification reaction was performed with MuscaFMRF-R1 and AAP primers, and nested PCR was carried out with a newly designed *Musca fmrf* gene-specific primer MuscaFMRF-R0 (5′-AGCCCATGCGACCCACTGAGCTC TT-3′ corresponding to the nucleotide sequence 670–694 in Fig. 1) and AUAP. All other reactions were executed as mentioned earlier.

In situ Hybridization of fmrf mRNA Gene—Fixation of Musca Brains—Brains of 5-day-old houseflies *Musca domestica* were dissected under a binocular microscope and fixed in freshly made 4% formaldehyde, as paraformaldehyde, in 0.1 M phosphate buffer (pH 7.4) for 12 h at 4°C. Tissues were washed at 4°C with 0.01 M PBS containing 0.1% Tween 20 (denoted as PBST), dehydrated with a series of MeOH solutions (25, 50, 75% and then 2 × 100%) in PBST, and stored at −20°C until use.

Preparation of cRNA Probes for Musca fmrf and pdf mRNA Genes—To clarify the location of the cells expressing *fmrf* mRNA, a digoxigenin (DIG)-labelled *fmrf* cRNA probe was prepared. Using T7 RNA polymerase, an antisense *fmrf* cRNA probe labelled by digoxigenin (DIG)-UTP was produced *in vitro* from plasmid linearized with *Sal*I. The plasmid used involved the PCR product corresponding to *fmrf* cDNA of position 1159–1592 in the vector pBluescript II SK+. The reaction mixture of plasmid (1 μg), 5× buffer (4 μl; 0.2 M Tris–HCl (pH 8.0), 40 mM $MgCl_2$, 10 mM spermidine-$(HCl)_3$, 125 mM NaCl), 10× DIG RNA labelling mix (2 μl; 10 mM ATP, 10 mM CTP, 10 mM GTP, 6.5 mM UTP, 3.5 mM DIG-11-UTP (pH 7.5; Roche Diagnostics, Mannheim, Germany), 5 mM DTT (2 μl), an RNase inhibitor RNasin® (1 μl; Promega, Madison, WI, USA) and T7 RNA polymerase for antisense primer (2 μl, 100 U) was incubated at 37°C for 2 h. The reaction was terminated by adding 0.5 M EDTA (2 μl, pH 8.0). In order to precipitate DIG-labelled cRNA product, 4 M LiCl (2 μl) and ethanol (75 μl) was added and the solution was centrifuged at 17,000*g* for 20 min at 4°C. The residual pellet was washed with 70% ethanol and dried in the air. The pellet was eventually dissolved in 50% formamide (50 μl). The quality of the transcript was analysed by electrophoresis on a 1.5% agarose gel stained with ethidium bromide.

For double-labelled *in situ* hybridization, DIG-labelled *fmrf* cRNA prepared above was utilized as one of the probes. In addition, as a counterprobe, a fluorescein isothiocyanate (FITC)-labelled *pdf* cRNA probe was prepared. Using T7 RNA polymerase, antisense *pdf* cRNA probe labelled with FITC-UTP was prepared *in vitro* from the plasmid linearized with *Bam*HI, corresponding to the nucleotide positions 39–501 of *Musca pdf* (GenBank accession No. AB095922). *In vitro* transcription was performed using an FITC RNA labelling mix (Roche) instead of the DIG RNA labelling mix.

Whole-mount in situ Hybridization—Whole-mount *in situ* hybridization was performed essentially as described by Wilkinson (*30*) with several significant modifications. All the following procedures were performed at 25°C unless otherwise noted. Dehydrated tissues were rehydrated through a reverse series of MeOH–PBST solutions (75, 50, 25% MeOH, and 2× PBST). These re-hydrated tissues were permeabilized with 10 μg/ml proteinase K (Nacalai Tesque, Kyoto) at 37°C for 15 min, washed with aqueous glycine (2 mg/ml) for 5 min, and then washed twice with PBST. They were fixed in 0.2% glutaraldehyde/4% paraformaldehyde in PBST for 20 min, washed twice with PBST and incubated in PBST at 70°C for 50 min. After cooling on ice, tissues were treated with 6% H_2O_2 for 1 h, washed three times with PBS and incubated with pre-hybridization buffer (50% formamide, 5× SSC (pH 4.5), 1% SDS, 50 μg/ml yeast tRNA and 50 μg/ml heparin) at 70°C for 1 h. The pre-hybridization buffer was then replaced with hybridization buffer, *i.e.* a solution of pre-hybridization buffer containing a DIG-labelled cRNA probe, and the solution was incubated at 70°C for 16 h.

After hybridization, tissues were washed three times with solution I [50% formamide, 5× SSC (pH 4.5) and 1% SDS] at 70°C for 30 min, and once more with a 1:1 mixture of solutions I and II (solution II: solution I with no formamide) at 70°C for 10 min. The tissues were washed further three times with solution II for 5 min, and then incubated with solution II for 20 min. Washings were repeated twice with solution III [50% formamide, 2× SSC (pH 4.5) and 1% SDS] for 5 min at 70°C, three times more with solution III, but for 30 min each, and then with a TBST solution in which Tris-buffered saline (TBS; 150 mM NaCl, and 100 mM Tris–HCl, pH 7.5) contains 1% Tween 20. After blocking at 25°C for 1 h, in order to visualize mRNA-bound probe by immunocytochemical detection, tissues were treated with Fab fragments of sheep anti-DIG antibody directly conjugated to alkaline phosphatase (AP). This incubation was continued for 16 h at 4°C. Tissues were then washed successively four times with TBST for 5 min each and seven times for 1 h each. After washing twice with NTMT [100 mM NaCl, 100 mM Tris–HCl (pH 9.5), 50 mM $MgCl_2$ and 1% Tween 20] for 5 min, the antibody detection

reaction was performed by incubating the tissues in the substrate solution [NTMT with 0.33 mg/ml 4-nitro-blue tetrazolium chloride (NBT) and 0.17 mg/ml 5-bromo-4-chloro-3-indolylphosphate, BCIP] for 30 min in shaded light, and finally washed with TBST. Finally, whole tissues were mounted in glycerol–gelatin (Sigma, St Louis, MO, USA) and observed by light microscopy with an Olympus BX50.

Double-labelled in situ Hybridization—Double-labelled *in situ* hybridization was performed by means of the procedure used for whole-mount *in situ* hybridization with some modifications. Housefly brains were incubated in the hybridization solution containing both DIG-labelled *fmrf* cRNA probe and FITC-labelled *pdf* cRNA probe for 16 h at 70°C. After this hybridization reaction, tissues were washed as described for the whole-mount *in situ* hybridization and brains were subjected to the blocking reaction. After blocking at 25°C for 1 h, tissues were treated with anti-DIG-peroxidase (POD) Fab fragments (Roche) for 16 h at 4°C. Tissues were washed and DIG-labelled *fmrf* cRNA signals were amplified by TSA™ plus dinitrophenol (DNP) technology. Briefly, tissues were treated with DNP working solution for 10 min and washed. After blocking, tissues were incubated with anti-DNP-HRP Fab fragments and signals were visualized by the ImmunoPure® Metal Enhanced DAB (dimethylaminoazobenzene) Substrate kit (Pierce), which utilizes cobalt chloride and nickel chloride to produce a dark-brown precipitate in the presence of horseradish peroxidase (HRP). After washing with TBST, housefly brains were incubated with anti-FITC-AP Fab fragments for 16 h and then with the substrate solution (NTMT containing BCIP/NBT) for 30 min in shaded light. Eventually, the whole tissues were washed with TBST and mounted in glycerol–gelatin (Sigma) to observe by light microscopy as before.

Double-labelled in situ Hybridization of Drosophila fmrf and pdf mRNA Genes—Double-labelled *in situ* hybridization of *Drosophila* (Canton S) *fmrf* and *pdf* mRNA genes was carried out using a DIG-labelled *fmrf* cRNA probe and an FITC-labelled *pdf* cRNA probe, respectively. Antisense *pdf* cRNA probe labelled with FITC-UTP was prepared *in vitro* from the phagemid linearized with *Eco*RI. This ca. 600 bp probe corresponds to the whole *Drosophila pdf* mRNA (GenBank accession No. NM079793). Antisense *fmrf* cRNA probe labelled by DIG-UTP was prepared in a similar way from plasmid involving the PCR product corresponding to *Drosophila fmrf* cDNA (GenBank accession No. NM139501) of position 656–1473. Fixation followed by double-labelled *in situ* hybridization was performed under the same conditions for *Musca*.

RESULTS

Musca domestica fmrf cDNA—Degenerate primers for cDNA cloning were designed with reference to the sequence homology between FMRFamide peptides of *Drosophila* and *Calliphora vomitoria* (*28*, *31*, *32*). For the 3′ RACE method, three primers, PKQDFMRFG-F, QDFMRFGR-F and DNFMRFGR-F, were used to amplify the *Musca fmrf* gene. Several distinct gel bands were detected in each PCR reaction using these primers, and the nucleotide sequences of all the resulting products were analysed. In short, only when DNFMRFGR-F was used the fragment of *Musca fmrf* gene was obtained and this product was found to contain five copies of FMRF (corresponding to 274–325 in the final amino acid sequence). 3′ RACE and 5′ RACE experiments were performed on the basis of sequence information of this fragment.

A full-length cDNA clone was finally obtained, and the entire oligonucleotide structure was clarified. It comprises 1640 bp encoding a precursor protein of 388 amino acid residues (Fig. 1). Since the selected ATG codon and its adjacent nucleotide sequences fulfilled Kozak's consensus motif (*33*), the initiator codon ATG was assigned to position 214–216 as shown in Fig. 1. No additional ATG codon was found in the upstream 5′ UTR region. The program Signal P (http://www.cbs.dtu.dk/services/SignalP/) for predicting a signal peptide cleavage site showed that 21 amino acids from a selected Met should be a signal peptide.

Amino Acid Sequence Analysis of FMRFamide Peptides—The amino acid sequence converted from the oligonucleotide sequence of the *Musca fmrf* cDNA gene revealed that the gene encodes 17 FaRPs in total. At the most C-terminal side, the precursor contains a C-terminal free 14-mer peptide. At the N-terminal side, there is a 101-mer peptide (or protein) truncated by the 22-mer N-terminal signal peptide and the KR cleavage site. Consecutively, there follow an 11-mer peptide amide LRSLQENAMRW-NH_2(GKR) and then an 18-mer peptide amide SYESYOLNRNGL ADKSSV-NH_2(GR). All 17 FaRPs are present between this 18-mer peptide amide and C-terminal 14-mer peptide. They are encoded in tandem, being truncated by the amidation signal of GR at 16 sites and GK at one site (Fig. 2). As shown in Fig. 2, the size of the *Musca* FaRPs is relatively small, with amino acid residues 7–21.

Among total of 17 copies of FaRPs, there are four copies of NPGSQDFMRF-NH_2(GR) and two copies of SPGSQDFMRF-NH_2(GR) (Fig. 2). Interestingly, these peptides have exactly the same sequence of PGSQ DFMRF-NH_2(GR), and only the N-terminal amino acids N(=Asn) and S(=Ser) are different from each other. When we designate these peptides NPGSQDFMRF-NH_2(GR) and SPGSQDFMRF-NH_2(GR) as (*N*) and (*S*), respectively, they were found to be encoded successively in tandem as in the order of (*S*)–(*N*)–(*S*)–(*N*)–(*N*)–(*N*). Other 11 of the FaRPs have an N-terminal peptide sequence of MGFLSNHQVIRDSRGDN, SVGGSGGN DDN, ASGSSD, AGQDN, AAGQD, GSGQD, ASGGQD, APSGQD, PDN, TPAQSSD or TPTQSSD, as well as the C-terminal FMRF-NH_2(GR). In *D. melanogaster*, 8 different kinds of FaRPs, which total 13 copies, are encoded in a single gene (Fig. 2). Among them, only PDNFMRF-NH_2(GR) was found to be shared between the *Drosophila* and *Musca* FaRPs.

fmrf-Expressing Cells in Musca Brains—Whole-mount *in situ* hybridization was performed to identify the cells expressing *fmrf* mRNA. A DIG-labelled cRNA probe

Fig. 2. **Various FMRFamide-related peptides present in the precursor proteins of the housefly *Musca domestica* (A) and the fruit fly *Drosophila melanogaster* (B).** The signal peptides shown by dotted underline were predicted by program Signal P (http://www.cbs.dtu.dk/services/SignalP/). Dibasic amino acid cleavage sites KR are double-underlined. All 'FMRF' sequences are boxed. A solo 'GK' sequence present in *Musca* FMRF amide is underlined. Asterisks indicate a stop codon there.

was prepared to hybridize the *fmrf* mRNA gene at positions 1159–1592, which corresponds to the 3′ portion (1159–1380) of the protein-coding region and 3′ UTR (1381–1592). As shown in Fig. 3A, approximately four cell groups were identified for the *Musca* brain by this whole-mount *in situ* hybridization procedure. One large group, with two cell clusters each containing two large cells, was observed in the lateral neurons in each optic lobe (Fig. 3B), and two slightly bigger cells were observed on both sides of the tritocerebrum (Fig. 3C). A cell group of about 14 fairly small cells was observed in the dorsal area (Fig. 3D), while another group of 13 cells was in the subesophageal ganglion (Fig. 3E). The arrangement of these clusters is summarized in Fig. 4. In addition to the lateral neurons, most *fmrf* mRNAs are expressed in the central brain. No signals were detected when used sense *fmrf* mRNA probe as negative control (data not shown).

It is significant that some *Musca fmrf* mRNA-expressing cells appeared to locate in the same portion of the brain as in the *Musca* brain, containing *Musca pdf* mRNA-expressing cells. As previously reported (*13*), these are the lateral neurons of the optic lobe. There are two *pdf* expressing cell clusters in each optic lobe, one comprising four large cells and the other four small cells, as seen with double-labelled *in situ* hybridization, below. The results from *in situ* hybridization of *fmrf* mRNA show that the two *fmrf*-expressing cell clusters are located among the lateral neurons and that their cell sizes are similar to those of the large *pdf*-expressing cells.

Double-labelled in situ Hybridization of fmrf- and pdf-expressing Cells—In situ hybridization experiments carried out individually to detect *fmrf* and *pdf* mRNAs, raised the possibility that, among the *fmrf*-expressing cells, two pairs of lateral neurons could also express *pdf* mRNA (Fig. 4). To confirm whether or not *fmrf* and *pdf* mRNAs are co-expressed in the exact same cells, double-labelled *in situ* hybridization was performed using the DIG-labelled cRNA probe to detect *fmrf* mRNA and FITC-labelled cRNA probe for *pdf* mRNA (Fig. 5A). Both signals were found in the same region of fly's brain containing the lateral neurons, the anterior cortex of the medulla. However, as shown in Fig. 5B,

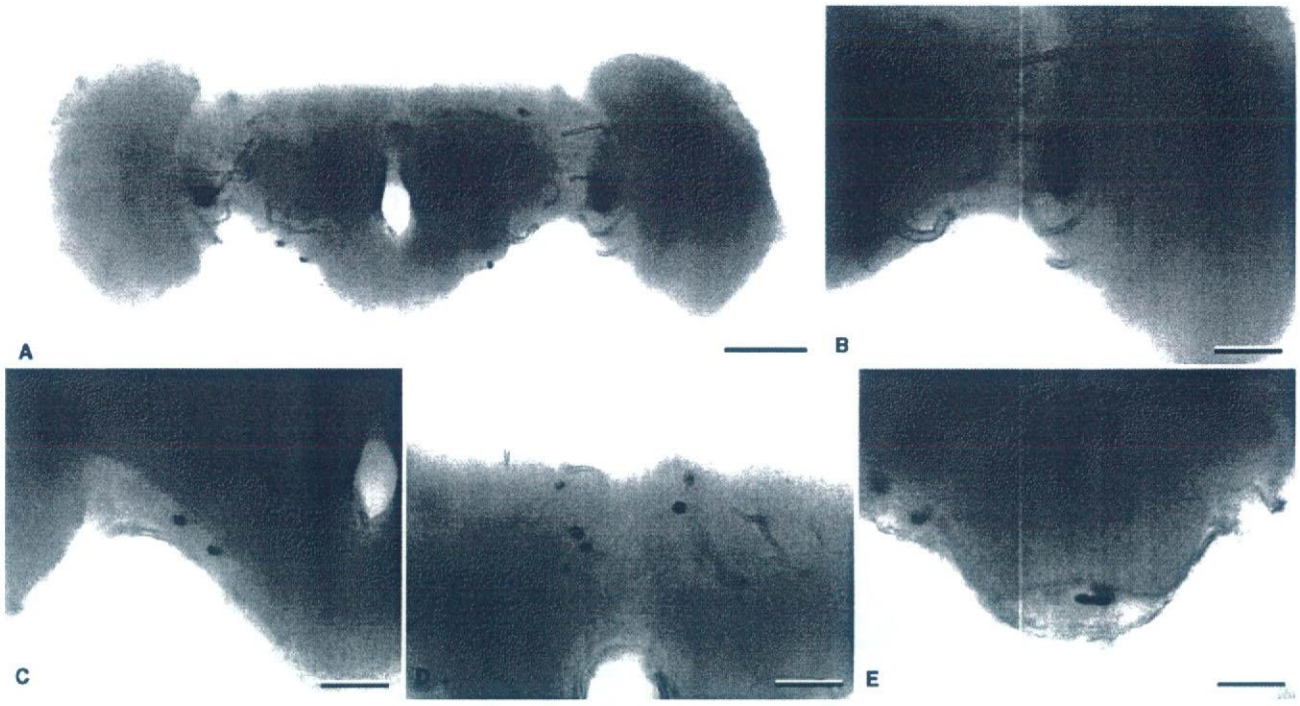

Fig. 3. **The whole-mount *in situ* hybridization for detection of *fmrf* mRNA in the brain of the housefly *Musca domestica*.** (A) A profile of whole brain with optic lobes (scale bar, 100 μm); and (B), (C), (D) and (E) expanded segmental views (scale bar, 50 μm). Observed cells are as follows: (B) two distinct cells in the lateral neurons in each optic lobe; (C) a single cell in the tritocerebrum; (D) approximately 14 cells in the dorsal area and (E) approximately 13 cells in the subesophageal ganglion.

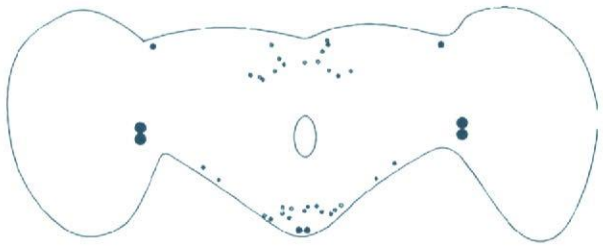

Fig. 4. **Schematic perspective drawing of the *fmrf* mRNA-expressing cells in the brain of the housefly *Musca domestica* detected by whole-mount *in situ* hybridization.** There are two pairs of four large cells among the lateral neurons, and two slightly bigger cells in the tritocerebrum. In addition, approximately 14 small cells are in the dorsal portion.

both brown and dark-blue signals never merged with each other. Two *fmrf*-expressing cells and all of *pdf*-expressing cells, four large and four small cells, were identified separately and individually in the lateral neurons. The *fmrf*-expressing cells revealed by brown signals were found more ventrally than the large *pdf*-expressing cells shown by dark-blue signals, and more lateral and dorsally than the small *pdf*-expressing cells. Given that the two signals nowhere merged, the *fmrf*-expressing cells are clearly different from the *pdf*-expressing cells.

The brains of *D. melanogaster* also exhibited non-merging signals of the *fmrf* mRNA hybridized by DIG-labelled cRNA probe and of the *pdf* mRNA hybridized by FITC-labelled cRNA probe. As shown in Fig. 6, with the FITC-labelled cRNA probe, *Drosophila pdf* mRNAs were observed in both large and small lateral neurons (*l*LNs and *s*LNs). When hybridized with DIG-labelled cRNA probe, *fmrf* mRNA-expressing cells were also found in the same region of the brain as the *pdf* mRNA-expressing *l*LNs and *s*LNs. However, again, the respective signals never merged, indicating that *fmrf*-expressing cells are clearly different from *pdf*-expressing cells.

DISCUSSION

Multiplicity of FMRFamide Peptides in the Amino Acid Sequence—Since the discovery of tetrapeptide FMRFamide, numerous members of the FaRP peptide family have been identified throughout the Metazoa. The *fmrf* mRNA was first clarified from an abdominal ganglion cDNA library of the marine mollusk *Aplysia californica* by a differential screening technique (*25*). Surprisingly, in addition to the FLRF tetrapeptide amide (=FLRFGR) and GYLRF pentapeptide amide (GYLRFGR), it encoded 28 FMRFs, the tetrapeptide amide FMRFGR, in tandem in a single gene. Multiple FaRPs are also encoded in other invertebrates, for instance, in the nematode *Caenorhabditis elegans*. *C. elegans* has no less than 20 FaRP precursor genes which encode a total of 56 FaRPs (*34*, *35*). No physiological significance of such diversity and multiplicity has yet been clarified.

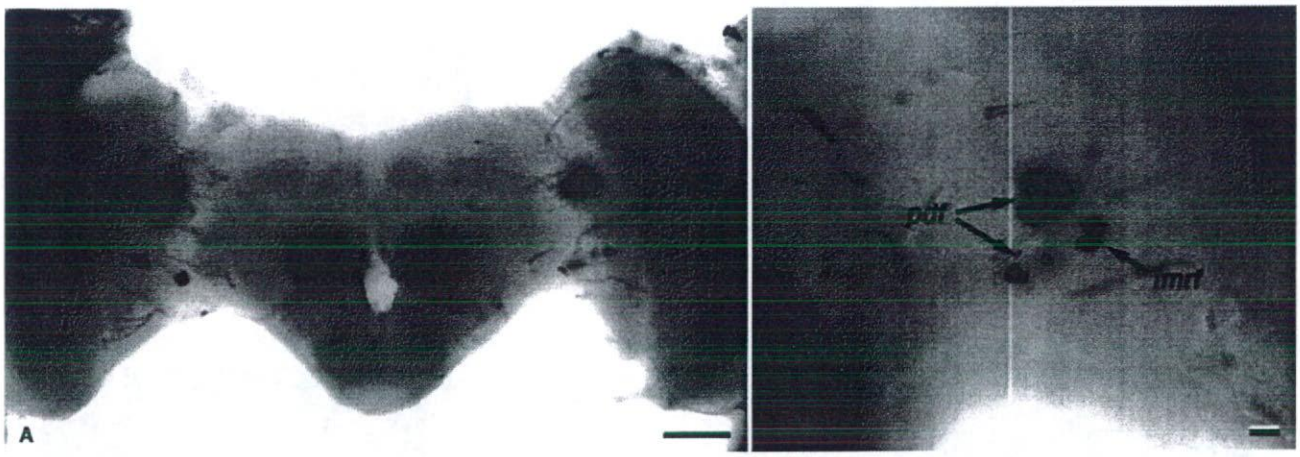

Fig. 5. **Double-labelled *in situ* hybridization of *fmrf* and *pdf* mRNAs in the brain of the housefly *Musca domestica*.** Brown signal indicates cells expressing *fmrf* mRNA, while dark-blue signal indicates those expressing the *pdf* mRNA. (A) Entire brain treated with double-labelled *in situ* hybridization (scale bar, 100 μm); and (B) expanded sectional view (scale bar, 20 μm).

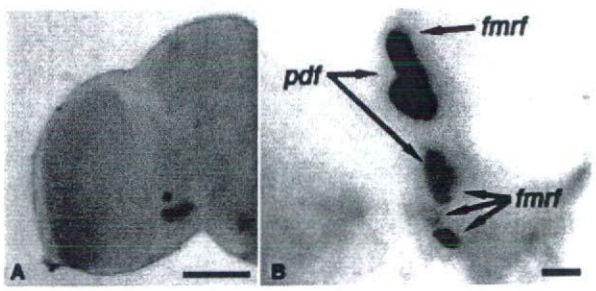

Fig. 6. **Double-labelled *in situ* hybridization of *fmrf* and *pdf* mRNAs in the brain of the fruit fly *Drosophila melanogaster*.** Brown signal indicates cells expressing *fmrf* mRNA, while dark-blue signal indicates those expressing the *pdf* mRNA. (A) Entire brain treated with double-labelled *in situ* hybridization (scale bar, 100 μm); and (B) expanded sectional view (scale bar, 20 μm).

In the EMBL/Genbank database, only two nucleotide sequences for FMRFamide peptides have been reported, the mRNAs of the fruit flies *D. melanogaster* and *D. virilis*. Indeed, such very limited information regarding the oligonucleotide sequences provided severe obstacles to the cDNA cloning of the housefly *fmrf* mRNAs, and required very sophisticated experimental strategies and primer design for the eventual successful cloning. For sufficient gene amplification, PCR should be carried out under the condition that there is an adequate number of target clones in the cDNAs that are reverse-transcribed. It was therefore a concern that the concentration of *fmrf* mRNA in the whole brain. In order to overcome this intrinsic problem, mRNAs were finally extracted from the thoracic ganglia. The fact that thirteen different FaRP peptides were actually isolated from the thoracic ganglia of the blowfly *Calliphora vomitoria* (*28*) prompted us to excise this tissue rather than the brain for the collection of concentrated *fmrf* mRNA. The difficulty in cDNA cloning further became clear when the amino acid sequence of the precursor protein of FMRFamide peptides was explored. Its sequence, particularly the sequences of FMRFamide peptides, was found to differ considerably from those of *D. melanogaster* (Fig. 7). The differences were remarkable; with only one FMRFamide peptide conserved between the two fly species, even though both are members of closely related clades of Diptera. It is evident that cDNA cloning of such a divergent gene is difficult.

When the amino acid sequences of precursor proteins translated from *Drosophila* and *Musca fmrf* mRNAs were compared (Fig. 2), these FaRP genes were found to show various disparities. First of all, the total numbers of copies of FMRFamide-containing peptides encoded in a single gene are different: 10 copies for *Drosophila* and 17 for *Musca*. Among the 17 *Musca* FMRFamide peptides, the peptides encoded at the most N-terminal side are 21- and 16-mer FMRFamides. All other FMRFamide peptides are rather short with 7–11 amino acid residues. Most FMRFamide peptides are truncated by GR at the both the N- and C-terminal sides, whereas the GR and GK sites truncate the most C-terminal TPTQSSDFMRFamide. Thus, there are 16 FMRFGR sequences in total and 1 FMRFGK in the same gene. Although the monobasic sites GR and GK are not always enzymatically cleavable (*36*), these are assumed to be the truncate sites for exclusive production of FMRFamide peptides. *Drosophila* has one longer-type (16-mer) and nine shorter-type (7–9-mer) FMRFamide peptides as shown in Fig. 7.

As to the FMRFamide peptides of the shorter type, there are remarkable differences in their primary structures. *Musca* FMRFamide encodes eight different 10-mer peptides, which contain a hexapeptide amide of QDFMRFamide in their C-terminus. The *Drosophila* FMRFamide precursor consists of six different peptides terminating with C-terminal QDFMRFamide, but in 9-mer peptides. These suggest an important role for the physiological functions of the QDFMRFamide moiety, presumably as an address code to specify and bind to specific receptors.

fmrf-Expressing Cells do not Express pdf—PDF peptide in *D. melanogaster* is present in several cell clusters

```
DmelanogasterFMRF  MGIALMFLLALYQMQSAIHSEIIDTPN-YAGNSLQDADSQVSPS----QDNDLVDALLGN 55
DvililusFMRF       MGIALMFLLALYQMQSAIHSEIIETPSSYNDNSLLEAAAEEPNSRATASESDLLDGLMST 60
MuscaFMRF          MVAPLLVFLFSLQLCHTTSWAYVGGNS-LNSNSLHASYSEFPAGTSNEVPEDAANGQDDN 59
                   *  .*:.:*   *:  :     :   .  .***  : :: . .      .*  :.  ..

DmelanogasterFMRF  DQ-----------------TERAELEFRHPISVIGIDYSKNAVVLHFQKHGRKPRYKYDP 98
DvililusFMRF       DNP--------------NPEQQTELEFRYPISAIGIGYAKNSVVLRFQKHARKQNFKYDP 106
MuscaFMRF          DDSQLTEPNDNNAPLVQSIDDETEMQFPKPIQWVSIDHLRNSIILRFQNPTPKILNKLDP 119
                   *:                   :.:*::*  **. :.*.: :*:::*:**:   *   * **

DmelanogasterFMRF  ELEAKRRSVQDNFMHFGKRQAEQLPPEGSYAGSDELEGMAKRAAMDRYGRDPKQD-FMRF 157
DvililusFMRF       DYEMKRKSLQDNFMHFGKRQAEQLP-QATGPG---YYECIKRSAMDRYGRDPKQD-FMRF 161
MuscaFMRF          EEMKRLRSLQENAMRWGKRSYESYPLNRNGLADKSSVGRMGFLSNHQVIRDSRGDNFMRF 179
                   :   : :*:*:* *::***. *. * : .  .          : .:  **.: * ****

DmelanogasterFMRF  GRDP------KQDFMRFGRDPKQDFMRFGRDPKQDFMRFGRDPKQDFMRFGRTPAADFMR 211
DvililusFMRF       GRAP------PSDFMRFGRAP--------------------------------SDFMR 181
MuscaFMRF          GRSVGGSGGNDDNFMRFGRASGSS----------DFMRFGRAGQDNFMRFGRAAGQDFMR 229
                   **         .:****** .                                 ****

DmelanogasterFMRF  FGRTPAEDFMRFGRS---DNFMRFGRSP--HEDVR---SP-KQDFMRFGR---PDNFMRF 259
DvililusFMRF       FGRDPSQDFMRFGRS---DNFMRFGRNLNFHEELR---SP-KQDFMRFGR---PDNFMRF 231
MuscaFMRF          FGRGSGQDFMRFGRSPGSQDFMRFGRNPGSQDFMRFGRSPGSQDFMRFGRNPGSQDFMRF 289
                   *** ..:********   ::******.   :: :*   ** .********   .::****

DmelanogasterFMRF  GRS-RPQDFVRSGK--MDSNFIRFGKS------LKPAAPESKPVKSNQGN--PGER---S 305
DvililusFMRF       GRS-APTEFERNGK--MDSNFMRFGKRSGVMAKLTKSQLQQNKLTTADGKQQPAEEG--N 286
MuscaFMRF          GRNPGSQDFMRFGRNPGSQDFMRFGRASGGQDFMRFGRAPSGQDFMRFGRPDNFMRFGRT 349
                   **.  . :* * *:   ..:*:***:       :  .  .       *.     .  .

DmelanogasterFMRF  PVDKAMTELFKKQELQDQ-------------QVKNGAQATTTQDGSVEQDQFFGQ 347
DvililusFMRF       PTDKAISMLFNKHQQQQQQQQGQRLQQEDRQQMKSSAEQNNLEEASVEQ--FYEP 339
MuscaFMRF          PAQSSDFMRFGRTPTQSS----------DFMRFGKSLDKSENKTSDLQK------ 388
                   *.:.:    * :   *..            :. .. : .  : ..:::
```

Fig. 7. **The sequence alignment of fly FMRFamide precursor proteins.** '*': Residues in that column are identical in all sequences in the alignment. ':': Conserved substitutions are observed. '.': Semi-conserved substitutions are observed.

of clock cells that express the clock gene *period*. There is clear evidence that the *pdf*-mutated flies show abnormal circadian rhythm behaviour (*11*), although these mutant flies do not show arrhythmic, completely random activity. Residual rhythmicity in *pdf* mutants and the residual *period*-expressing cells which lack *pdf* peptide likely reflects the activity of other neurotransmitters. It has also been reported that certain mosaic flies for the neuropeptide amidating enzyme were less rhythmic than *pdf* mutants (*37*). This suggests that multiple amidated neuropeptides other than PDF function in daily locomotor rhythms.

Together with these suggestions, several other investigations strongly suggested that (*1*) FMRFamide peptides are a neuropeptide involved in circadian rhythm (*20*); and (*2*) FMRFamide peptides are co-expressed or co-localized with PDF peptide in the same neurons (*20–23*). However, the latter possibility was clearly excluded in the present study by means of double-labelled *in situ* hybridization, at least for the two flies *M. domestica* and *D. melanogaster*. In *Musca* brains, a cell cluster of two *pdf*-expressing cells and two *fmrf*-expressing cells is present symmetrically in the lateral regions of each optic lobe. These *fmrf*-expressing cells and *pdf*-expressing cells lie in close proximity to each other, but apparently do not overlap or merge, and thus are different neurons. The same was also clear in the *Drosophila* brains.

Although double-immunolabelling in insect brains using anti-crustacean β-PDH and anti-FMRFamide antibody suggested that insect PDF and FMRFamide-like peptides might co-exist in the same cells (*20–23*), the present study demonstrated non-overlapping expression of *pdf* and *fmrf* mRNA genes. We analysed previously the specificity of anti-crustacean β-PDH antibody (*19*), and evidenced that the PDF-expressing neurons are the same cells detected by *in situ* hybridization (*16, 17*). The present results suggest possible cross-reactivity to unknown peptides of anti-FMRFamide antibody.

The mechanism of cell-specific transcriptional regulation of the *Drosophila fmrf* gene has been clearly

characterized (*38*). Transcriptional control elements required for spatial and temporal regulation of *fmrf* gene expression seem to be distributed over 8 kb of genomic DNA and several enhancer regions have been identified in the 5′ region of the *fmrf* gene. These cell-specific expression patterns presumably indicate the importance of the gene product, the multiple FaRPs in the insect nervous system, some of which perhaps function in circadian rhythms. If FMRFamide peptides were involved in the molecular mechanisms underlying circadian rhythms, they and their gene would be predicted to exhibit certain circadian prerequisites: for instance (*1*) peptides in secretary vesicles may exhibit a circadian rhythmicity; (*2*) mRNA may co-express in a neuron with *period* mRNA or (*3*) mRNA production may exhibit circadian rhythmicity. Experiments to reveal these points are in progress in our laboratory.

We thank Prof. Ian A. Meinertzhagen, Dalhousie University, Canada, for reading the manuscript. This study was supported by grants-in-aid from the Ministry of Education, Science, Sports and Culture in Japan; grant 11878113 to Y.S., and grant 1287115 & 18570075 to M.S., and in part by Health and Labour Sciences Research Grants for Research on Risk of Chemical Substances from the Ministry of Health, Labor and Welfare of Japan to Y.S.

REFERENCES

1. Price, D.A. and Greenberg, M.J. (1977) Structure of a molluscan cardioexcitatory neuropeptide. *Science* **197**, 670–671
2. Nichols, R., Schneuwly, S.A., and Dixon, J.E. (1988) Identification and characterization of *Drosophila* homologue to the vertebrate neuropeptide cholecystokinin. *J. Biol. Chem.* **263**, 12167–12170
3. Holman, G.M., Cool, B.J., and Nachman, R.J. (1986) Isolation, primary structure and synthesis of leucomyosuppressin, an insect neuropeptide that inhibits spontaneous contractions of the cockroach hindgut. *Comp. Biochem. Physiol.* **85C**, 329–333
4. Nichols, R. (1992) Isolation and structural characterization of *Drosophila* TDVDHVFLRFamide and FMRFamide-containing neural peptides. *J. Mol. Neurosci.* **3**, 213–218
5. Rao, K.R., Mohrherr, C.J., Riehm, J.P., and Zahnow, C.A. (1987) Primary structure of an analog of crustacean pigment-dispersing hormone from the lubber grasshopper *Romalea microptera*. *J. Biol. Chem.* **262**, 2672–2675
6. Stengl, M. and Homberg, U. (1994) Pigment-dispersing hormone-immunoreactive neurons in the cockroach *Leucophaea maderae* share properties with circadian pacemaker neurons. *J. Comp. Physiol.* [A] **175**, 203–213
7. Pyza, E. and Meinertzhagen, I.A. (1996) Neurotransmitters regulate rhythmic size changes amongst cells in the fly's optic lobe. *J. Comp. Physiol.* [A] **178**, 33–45
8. Meinertzhagen, I.A. and Pyza, E. (1996) Daily rhythms in cells of the fly's optic lobe: taking time out from the circadian clock. *Trends Neurosci.* **19**, 285–291
9. Mertens, I., Vandingenen, A., Johnson, E.C., Shafer, O.T., Li, W., Trigg, J.S., De Loof, A., Schoofs, L., and Taghert, P.H. (2005) PDF receptor signaling in *Drosophila* contributes to both circadian and geotaxic behaviors. *Neuron* **48**, 213–219
10. Petri, B. and Stengl, M. (1997) Pigment-dispersing hormone shifts the phase of the circadian pacemaker of the cockroach *Leucophaea maderae*. *J. Neurosci.* **17**, 4087–4093
11. Renn, S.C.P., Park, J.H., Rosbash, M., Hall, J.C., and Taghert, P.H. (1999) A *pdf* neuropeptide gene mutation and ablation of PDF neurons each cause severe abnormalities of behavioral circadian rhythms in *Drosophila*. *Cell* **99**, 791–802
12. Park, J.H., Helfrich-Föster, C., Lee, G., Liu, L., Rosbash, M., and Hall, J.C. (2000) Differential regulation of circadian pacemaker output by separate clock genes in *Drosophila*. *Proc. Natl. Acad. Sci. USA* **97**, 3608–3613
13. Helfrich-Förster, C., Täuber, M., Park, J.H., Muhlig-Versen, M., Schneuwly, S., and Hofbauer, A. (2000) Ectopic expression of the neuropeptide pigment-dispersing factor alters behavioral rhythms in *Drosophila melanogaster*. *J. Neurosci.* **20**, 3339–3353
14. Shirasu, N., Shimohigashi, Y., Tominaga, Y., and Shimohigashi, M. (2003) Molecular cogs of the insect circadian clock. *Zool. Sci.* **20**, 947–955
15. Chuman, Y., Matsushima, A., Sato, S., Tomioka, K., Tominaga, Y., Meinertzhagen, I.A., Shimohigashi, Y., and Shimohigashi, M. (2002) cDNA cloning and nuclear localization of the circadian neuropeptide designated as pigment-dispersing factor PDF in the cricket *Gryllus bimaculatus*. *J. Biochem.* **131**, 895–903
16. Matsushima, A., Yokotani, S., Lui, X., Sumida, K., Honda, T., Sato, S., Kaneki, A., Takeda, Y., Chuman, Y., Ozaki, M., Asai, D., Nose, T., Onoue, H., Ito, Y., Tominaga, Y., Shimohigashi, Y., and Shimohigashi, M. (2003) Molecular cloning and circadian expression profile of insect neuropeptide PDF in black blowfly, *Phormia regina*. *Lett. Pept. Sci.* **10**, 419–430
17. Matsushima, A., Sato, S., Chuman, Y., Takeda, Y., Yokotani, S., Nose, T., Tominaga, Y., Shimohigashi, M., and Shimohigashi, Y. (2004) cDNA cloning of the housefly pigment-dispersing factor (PDF) precursors protein and its peptide comparison among the insect circadian neuropeptides. *J. Pept. Sci.* **10**, 82–91
18. Sato, S., Chuman, Y., Matsushima, A., Tominaga, Y., Shimohigashi, Y., and Shimohigashi, M. (2002) A circadian neuropeptide, pigment-dispersing factor – PDF, in the last summer cicada *Meimuna opalifera*: cDNA cloning and immunocytochemistry. *Zool. Sci.* **19**, 821–828
19. Honda, T., Matsushima, A., Sumida, K., Chuman, Y., Sakaguchi, K., Onoue, H., Meinertzhagen, I.A., Shimohigashi, Y., and Shimohigashi, M. (2006) Structural isoforms of the circadian neuropeptide PDF expressed in the optic lobes of the cricket *Gryllus bimaculatus*: Immunocytochemical evidence from specific monoclonal antibodies. *J. Comp. Neurol.* **499**, 404–421
20. Pyza, E. and Meinertzhagen, I.A. (2003) The regulation of circadian rhythms in the fly's visual system: involvement of FMRFamide-like neuropeptides and their relationship to pigment dispersing factor in *Musca domestica* and *Drosophila melanogaster*. *Neuropeptides* **37**, 277–289
21. Homberg, U., Davis, N.T., and Hildebrand, J.G. (1991) Peptide-immunocytochemistry of neurosecretory cells in the brain and retrocerebral complex of the sphinx moth *Manduca sexta*. *J. Comp. Neurol.* **303**, 35–52
22. Nässel, D.R., Shiga, S., Mohrherr, C.J., and Rao, K.R. (1993) Pigment-dispersing hormone-like peptide in the nervous system of the flies *Phormia* and *Drosophila*: Immunocytochemistry and partial characterization. *J. Comp. Neurol.* **331**, 183–198
23. Settembrini, B.P. and Villar, M.J. (2005) FMRFamide-like immunocytochemistry in the brain and aubesophageal ganglion of *Triatoma infestans* (Insecta: Heteroptera). Coexpression with β-pigment-dispersing hormone and small cardioactive peptide. *Cell Tissue Res.* **321**, 299–310
24. Schaefer, M., Picciotto, R., Thane, K., Kaldany, R.R., Taussing, R., and Scheller, R.H. (1985) *Aplysia* neurons express a gene encoding multiple FMRFamide neuropeptides. *Cell* **41**, 457–467

25. Schneider, L.E. and Taghert, P.H. (1988) Isolation and characterization of a *Drosophila* gene that encodes multiple neuropeptides related to Phe-Met-Arg-Phe-NH_2 (FMRFamide). *Proc. Natl. Acad. Sci. USA* **85**, 1993–1997
26. Taghert, P.H. and Schneider, L.E. (1990) Interspecific comparison of a *Drosophila* gene encoding FMRFamide-related neuropeptides. *J. Neurosci.* **10**, 1929–1942
27. Frohman, M.A., Dush, M.K., and Martin, G.R. (1988) Rapid production of full-length cDNAs from rare transcripts: amplification using a single gene-specific oligonucleotide primer. *Proc. Natl. Acad. Sci. USA* **85**, 8998–9002
28. Duve, H., Johnsen, A.H., Sewell, J.C., Scott, A.G, Orchard, I., Rehfeild, J.F., and Thorpe, A. (1992) Isolation, structure, and activity of -Phe-Met-Arg-Phe-NH_2 neuropeptides (designated calliFMRFamides) from the blowfly *Calliphora vomitoria*. *Proc. Natl. Acad. Sci. USA* **89**, 2326–2330
29. Don, R.H., Cox, P.T., Wainwright, B.J., Baker, K., and Mattick, J.S (1991) 'Touchdown' PCR to circumvent spurious priming during gene amplification. *Nucleic Acids Res.* **19**, 4008
30. Wilkinson, D.G. (Ed.) (1999) *In Situ Hybridization: A Practical Approach*, 2nd edn, Oxford University Press, Oxford
31. Orchard, I., Lange, A.B., and Bendena, W.G. (2001) FMRFamide-related peptides: a multifunctional family of structurally related neuropeptides in insects. *Adv. Insect Physiol.* **28**, 267–329
32. Nässel, D.R. (2002) Neuropeptides in the nervous system of *Drosophila* and other insects: multiple roles as neuromodulators and neurohormones. *Prog. Neurobiol.* **68**, 1–84
33. Kozak, M. (1999) Initiation of translation in prokaryotes and eukaryotes. *Gene* **234**, 187–208
34. Li, C., Kim, K., and Nelson, L.S. (1999) FMRFamide-related neuropeptide gene family in *Caenorhabditis elegans*. *Brain Res.* **848**, 26–34
35. Li, C., Nelson, L.S., Kim, K., Nathoo, A., and Hart, A.C. (1999) Neuropeptide gene families in the nematode *Caenorhabditis elegans*. *Ann. N.Y. Acad. Sci.* **897**, 239–252
36. Veenstra, J.A. (2000) Mono- and dibasic proteolytic cleavage sites in insect neuroendocrine peptide precursors. *Arc. Insect Biochem. Physiol.* **43**, 49–63
37. Taghert, P.H., Hewes, R.S., Park, J.H., O'Brien, M.A., Han, M., and Peck, M.E. (2001) Multiple amidated neuropeptides are required for normal circadian locomotor rhythms in *Drosophila*. *J. Neurosci.* **21**, 6673–6686
38. Benveniste, R.J. and Taghert, P.H. (1999) Cell type-specific regulatory sequences control expression of the *Drosophila* FMRF-NH_2 neuropeptide gene. *J. Neurobiol.* **38**, 507–520